Mapping the Anisotropic Stochastic Gravitational-Wave Background

Jishnu Suresh

Université catholique de Louvain, Louvain-la-Neuve

Copernicus Webinar, January 31, 2023

GWTC: Gravitational Waves Transient Catalog - 3

arXiv
1811.12907
2108.01045
2111.03606

- 3 GW detection during O1
- First direct detection of GW
- From coalescing binary systems of black holes

- 8 GW detection during O2
- 1 coalescing binary system of neutron stars: electromagnetic counterpart detected

- 79 GW detection during O3
- 44 during O3a, including 1 confirmed binary system of neutron stars
- 35 during O3b, including 2 confirmed systems of neutron stars - black holes
- No electromagnetic counterpart

- O4 to start around May 2023
- Duration: 1.5 year

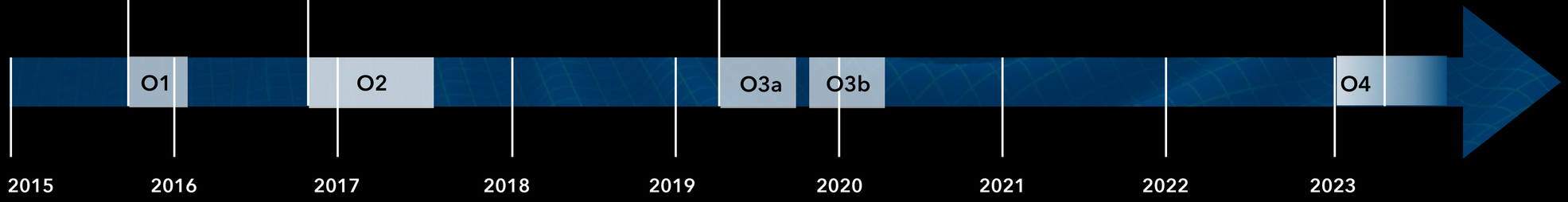

90 GW detections reported

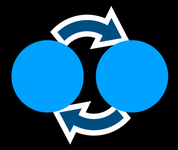

Coalescence of black holes and neutron stars

1 multimessenger event (GW + EM observation)

Mass range
1.2 → 107
M⊙(stellar)

Distance range
40 Mpc → 8 Gpc
(z → 1.14)

Credit: Leïla Haegel for the LVK collaboration [2022]

WHAT'S NEXT

Continuous

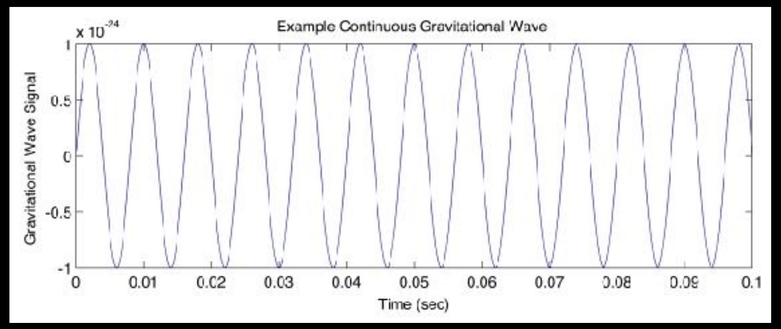

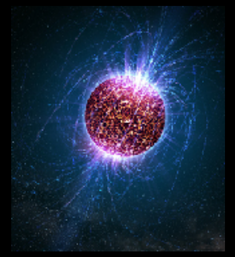

A single star swiftly rotating about its axis with a large mountain or other irregularity on it

Expected to produce comparatively weak gravitational waves

Inspiral

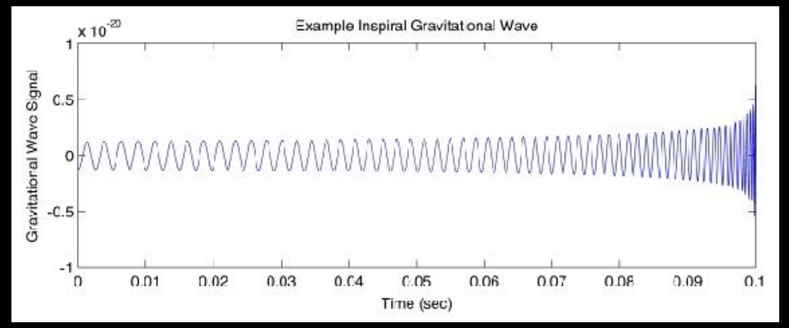

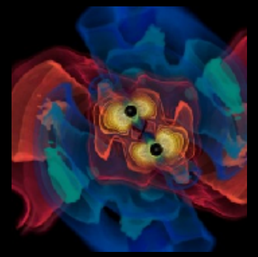

Generated during the end-of-life stage of binary systems where the two objects merge into one.

These systems are usually two neutron stars, two black holes, or a neutron star and a black hole

Burst

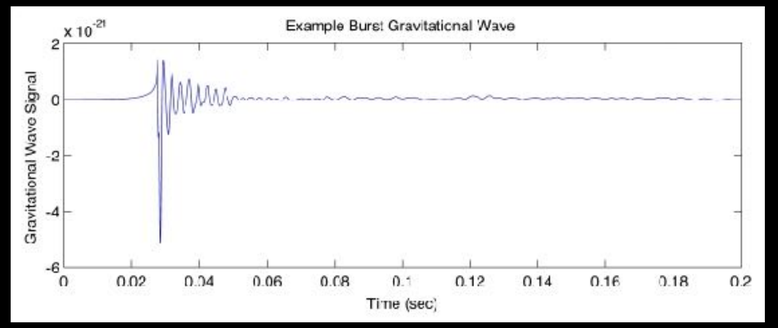

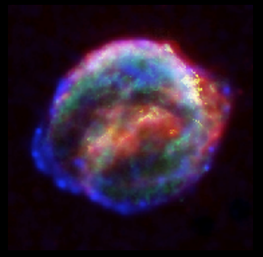

From short-duration unknown or unanticipated sources

There are hypotheses that some systems such as supernovae or gamma ray bursts may produce burst gravitational waves, but too little is known about the details of these systems to anticipate the form these waves will have

Stochastic Background

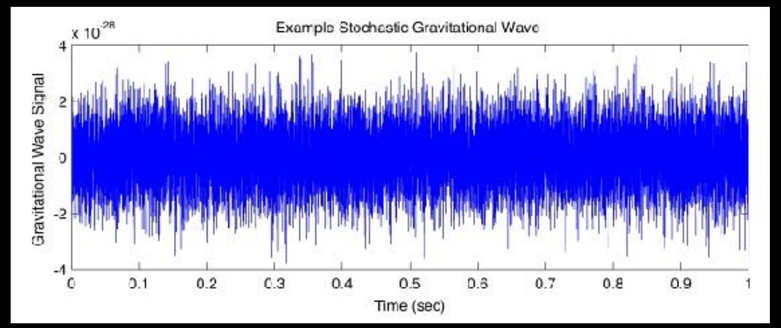

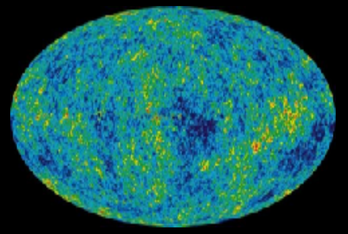

Incoherent superposition of many GW sources. It could be cosmological (for example, vacuum fluctuation from the early universe) and/or astrophysical (for example, adding contribution from all binary black hole coalescence in the universe).

WHAT'S NEXT

Continuous

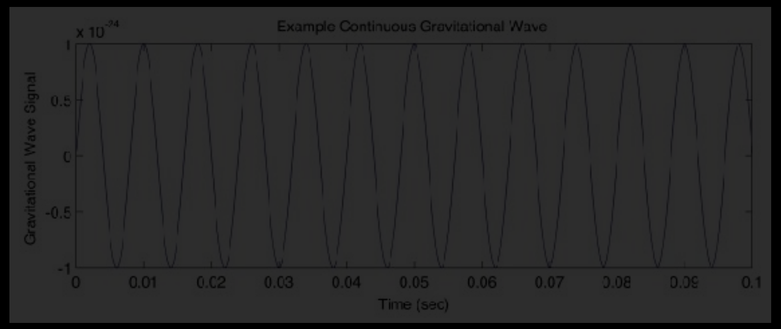

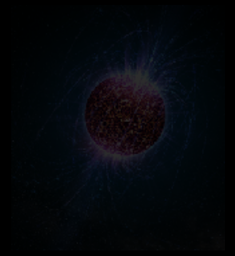

A single star swiftly rotating about its axis with a large mountain or other irregularity on it

Expected to produce comparatively weak gravitational waves

Inspiral

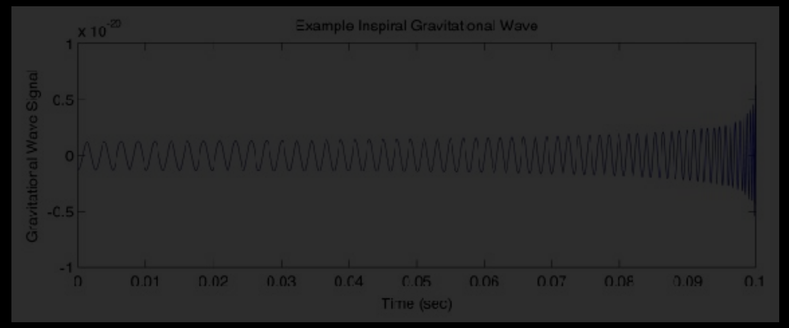

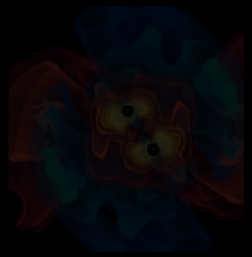

Generated during the end-of-life stage of binary systems where the two objects merge into one.

These systems are usually two neutron stars, two black holes, or a neutron star and a black hole

Burst

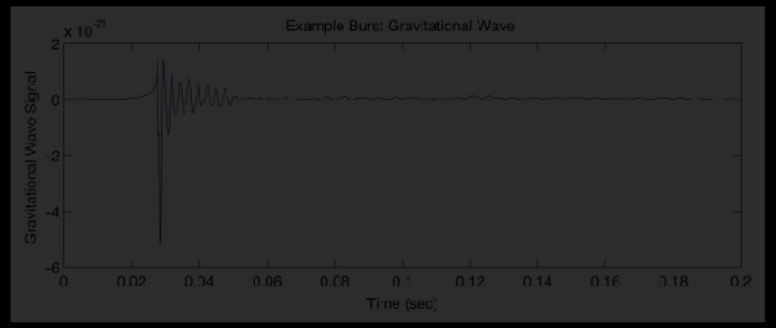

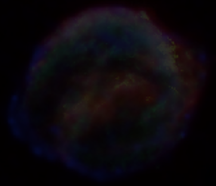

From short-duration unknown or unanticipated sources

There are hypotheses that some systems such as supernovae or gamma ray bursts may produce burst gravitational waves, but too little is known about the details of these systems to anticipate the form these waves will have

Stochastic Background

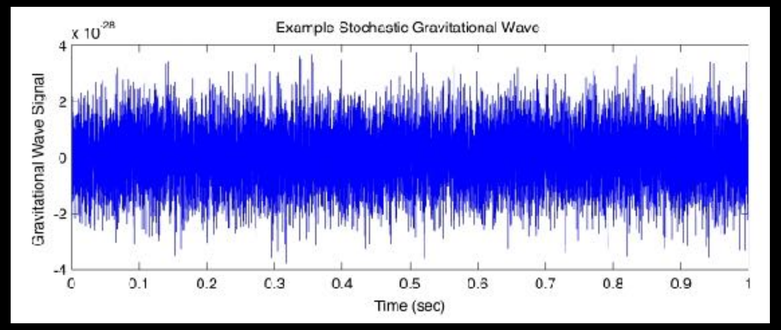

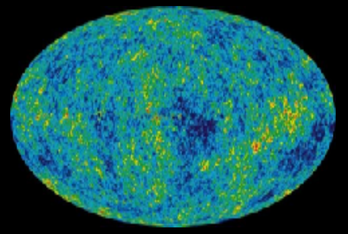

Incoherent superposition of many GW sources. It could be cosmological (for example, vacuum fluctuation from the early universe) and/or astrophysical (for example, adding contribution from all binary black hole coalescence in the universe).

STOCHASTIC GRAVITATIONAL WAVE BACKGROUND

Superposition of signals too weak or too numerous to individually detect

Looks like noise in a single detector

Characterized statistically in terms of moments (ensemble averages) of the metric perturbations

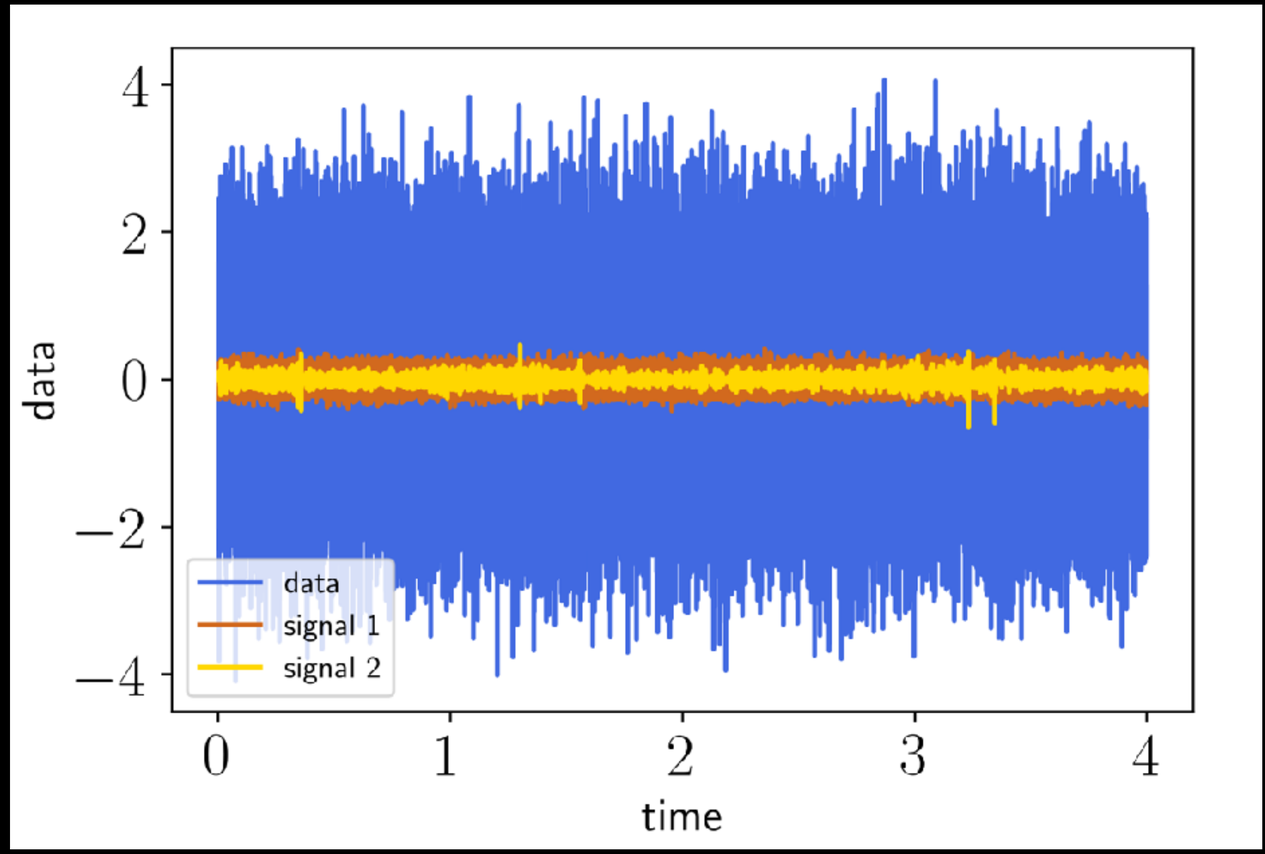

TYPES OF STOCHASTIC GRAVITATIONAL WAVE BACKGROUND

(i) Stochastic backgrounds can differ in spatial distribution

(statistically) isotropic

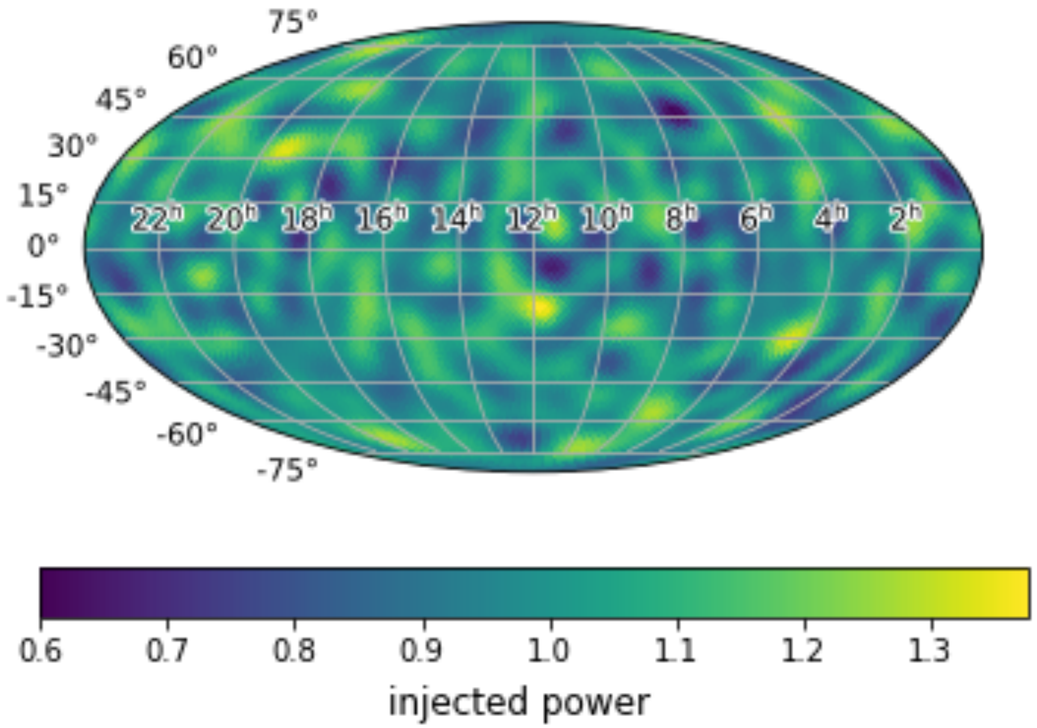

(like cosmic microwave background)

anisotropic

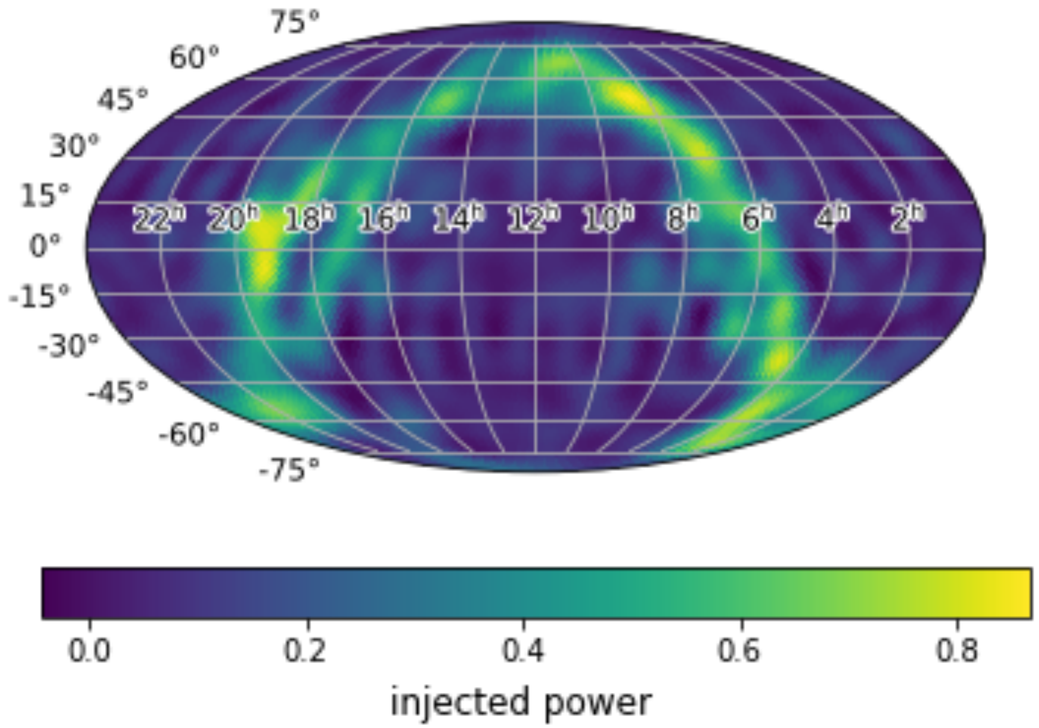

(galactic plane in equatorial coordinates)

(ii) They can also differ in temporal distribution and amplitude

Stationary Gaussian

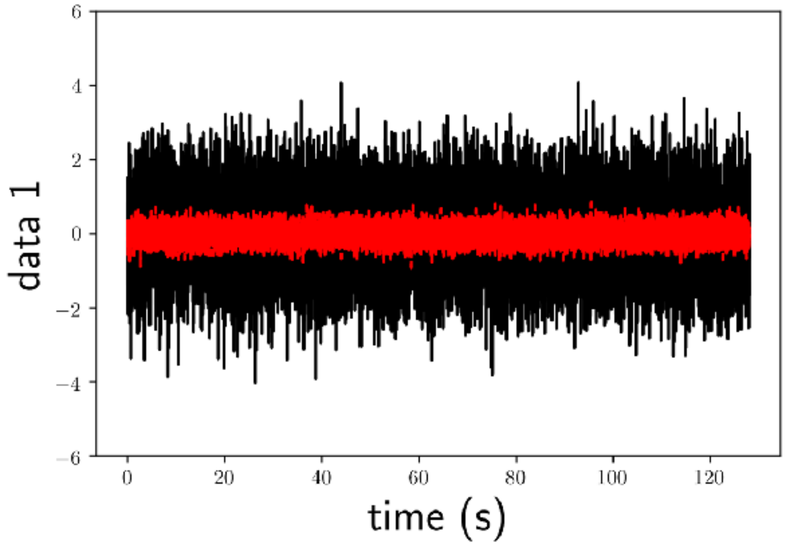

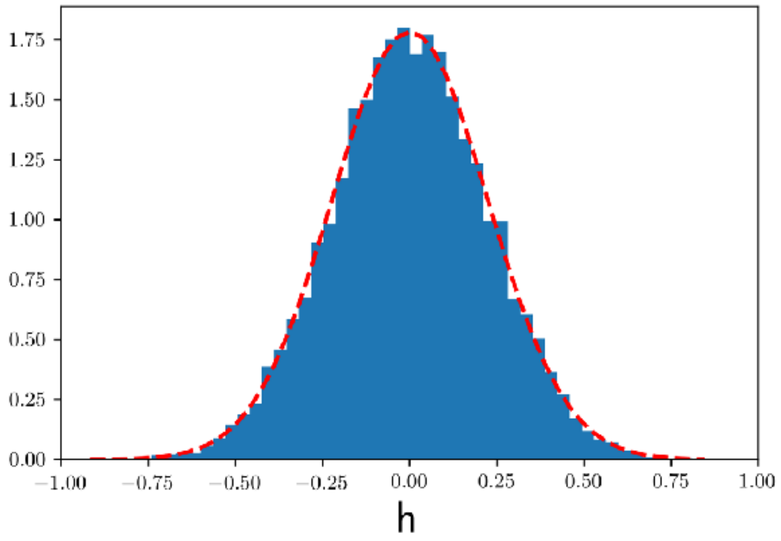

Non-stationary (non-gaussian)

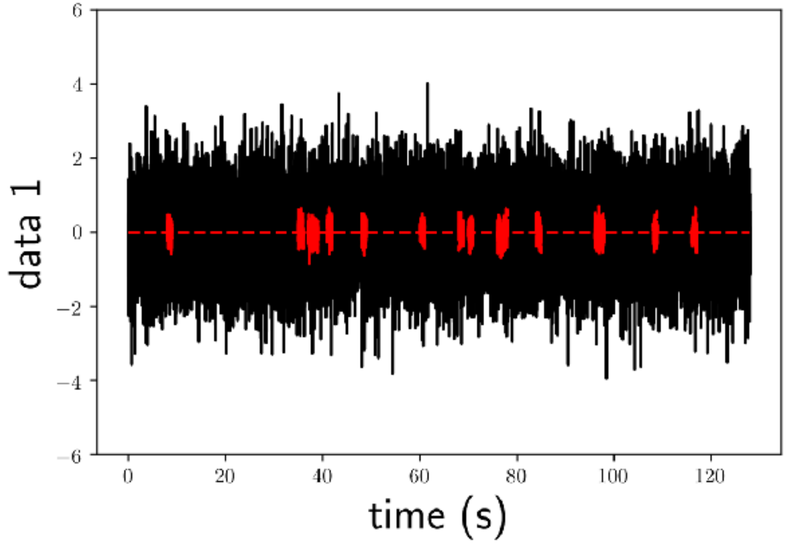

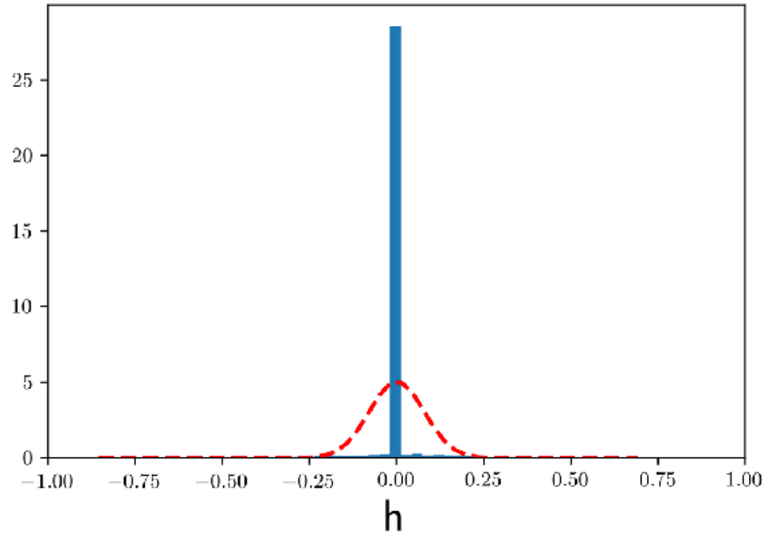

Foreground

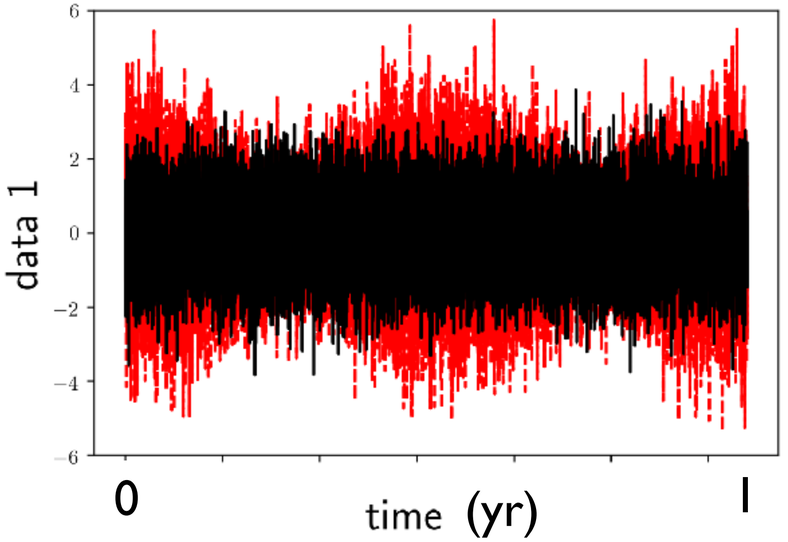

(e.g., from galactic white dwarf binaries; modulated by LISA's orbital motion)

(credit: J. Romano)

(iii) They can also differ in power spectra depending on source

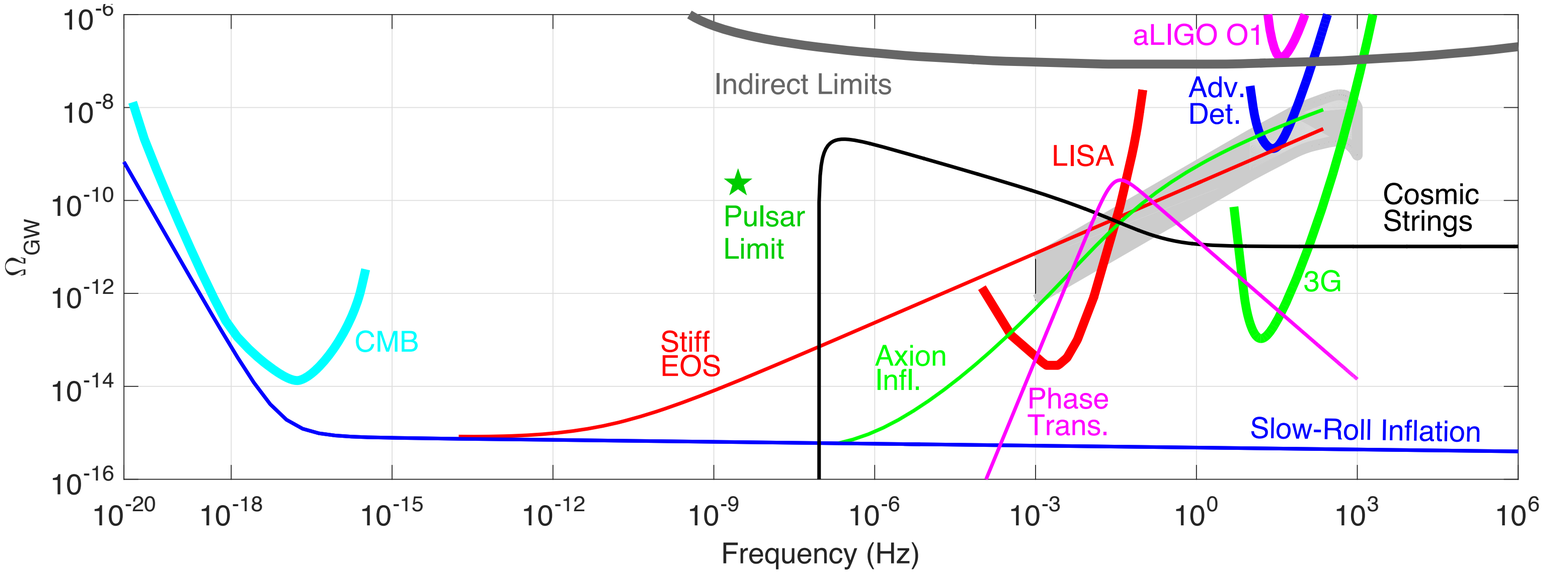

Overview of several proposed model spectra for cosmic SGWB and different experiments' sensitivities.

Taxonomy of astrophysical SGWB within the frequency range of ground-based detectors.

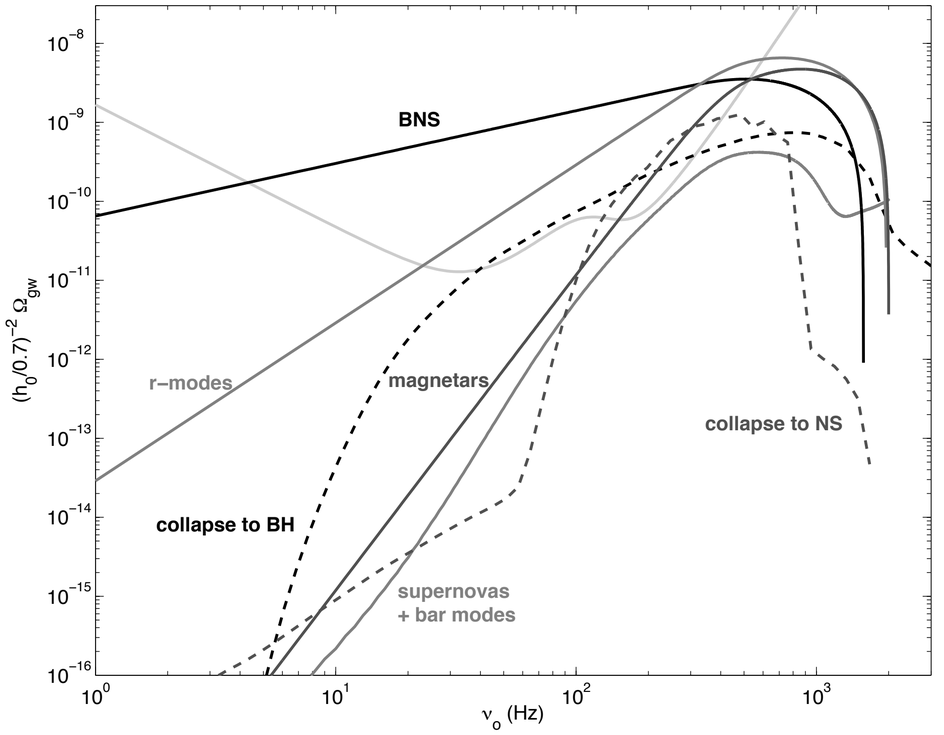

STOCHASTIC GRAVITATIONAL WAVE BACKGROUND

Plane wave expansion of metric perturbations

$$h_{ab}(t,\vec{x}) = \int_{-\infty}^{\infty} \mathrm{d}f \int \mathrm{d}^2\Omega_{\hat{n}} \sum_{A=+,\times} h_A(f,\hat{n}) e^A_{ab}(\hat{n})\, e^{i2\pi f(t+\hat{n}\cdot\vec{x}/c)}$$

Polarization tensors:

$$e^+_{ab}(\hat{n}) = \hat{l}_a\hat{l}_b - \hat{m}_a\hat{m}_b$$

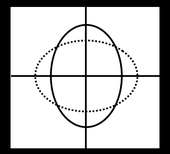

A=+

$$e^\times_{ab}(\hat{n}) = \hat{l}_a\hat{m}_b + \hat{m}_a\hat{l}_b$$

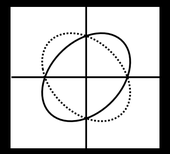

A=x

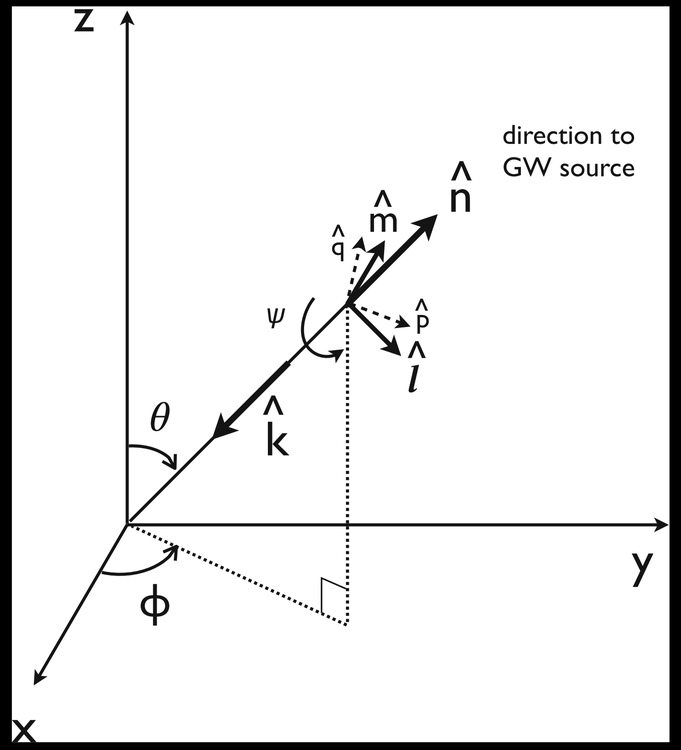

Statistical properties encoded in:

$$\langle h_A(f,\hat{n})\rangle\,, \quad \langle h_A(f,\hat{n}) h_{A'}(f',\hat{n}')\rangle\,, \quad \langle h_A(f,\hat{n}) h_{A'}(f',\hat{n}') h_{A''}(f'',\hat{n}'')\rangle\,, \quad \cdots$$

0

(no loss of generality)

in terms of quadratic expectation values

(if Gaussian)

STOCHASTIC GRAVITATIONAL WAVE BACKGROUND

Quadratic expectation values specify different types of Gaussian stochastic backgrounds

Unpolarized, stationary isotropic:

$$\langle h_A(f,\hat{n})\, h^*_{A'}(f',\hat{n}')\rangle = \frac{1}{16\pi} S_h(f)\, \delta(f-f')\delta_{AA'}\delta^2(\hat{n},\hat{n}')$$

Unpolarized, stationary, anisotropic:

$$\langle h_A(f,\hat{n})\, h^*_{A'}(f',\hat{n}')\rangle = \frac{1}{4} \mathscr{P}(f,\hat{n})\, \delta(f-f')\delta_{AA'}\delta^2(\hat{n},\hat{n}')$$

where $S_h(f) = \int \mathrm{d}^2\Omega_{\hat{n}}\, \mathscr{P}(f,\hat{n})$

power spectral density (Hz^{-1})

$$S_h(f) = \frac{3H_0^2}{2\pi^2}\frac{\Omega_{\rm gw}(f)}{f^3}$$

energy density spectrum (dimensionless)

$$\Omega_{\rm gw}(f) \equiv \frac{1}{\rho_c}\frac{\mathrm{d}\rho_{\rm gw}}{\mathrm{d}\ln f} = \frac{f}{\rho_c}\frac{\mathrm{d}\rho_{\rm gw}}{\mathrm{d}f}$$

characteristic strain (dimensionless)

$$h_c(f) \equiv \sqrt{f S_h(f)} = A_\alpha \left(\frac{f}{f_{\rm ref}}\right)^\alpha$$

STOCHASTIC GRAVITATIONAL WAVE BACKGROUND

Problem:

- The stochastic signal looks more like noise in a single detector.

Solutions:

- Identify features that distinguish between the expected signal and noise.
    - Know our GW detector's noise sources well enough in amplitude and spectral shape.
- For multiple detectors having uncorrelated noise: cross-correlation separates the signal from the noise.

STOCHASTIC GRAVITATIONAL WAVE BACKGROUND

Cross-correlation: basic idea

Data from two detectors:

$$d_1 = h + n_1$$
$$d_2 = h + n_2$$

common GW signal component

Expected value of cross-correlation:

$$\langle \hat{C}_{12} \rangle = \langle d_1\, d_2 \rangle = \langle h^2 \rangle + \langle n_1\, n_2 \rangle + \langle h\, n_2 \rangle + \langle n_1\, h \rangle = \langle h^2 \rangle + \langle n_1\, n_2 \rangle$$

$\langle h\, n_2 \rangle \to 0$, $\langle n_1\, h \rangle \to 0$

Assuming detector noise is uncorrelated:

$$\langle \hat{C}_{12} \rangle = \langle h^2 \rangle \equiv S_h$$

Detector response

GWs are weak => detector is a linear system which converts metric perturbations to detector output

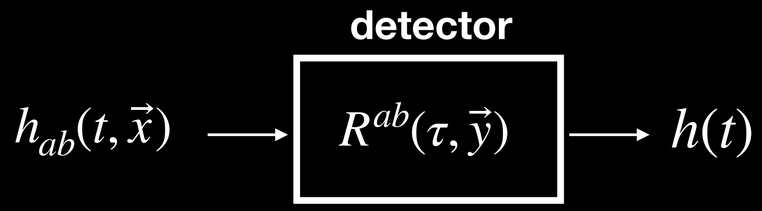

detector output $\Longrightarrow$ $\tilde{h}(f) = \int \mathrm{d}^2\Omega_{\hat{n}} \sum_A R^A(f,\hat{n})\, h_A(f,\hat{n})$

detector response for a plane-wave
with frequency f, direction n, polarization A

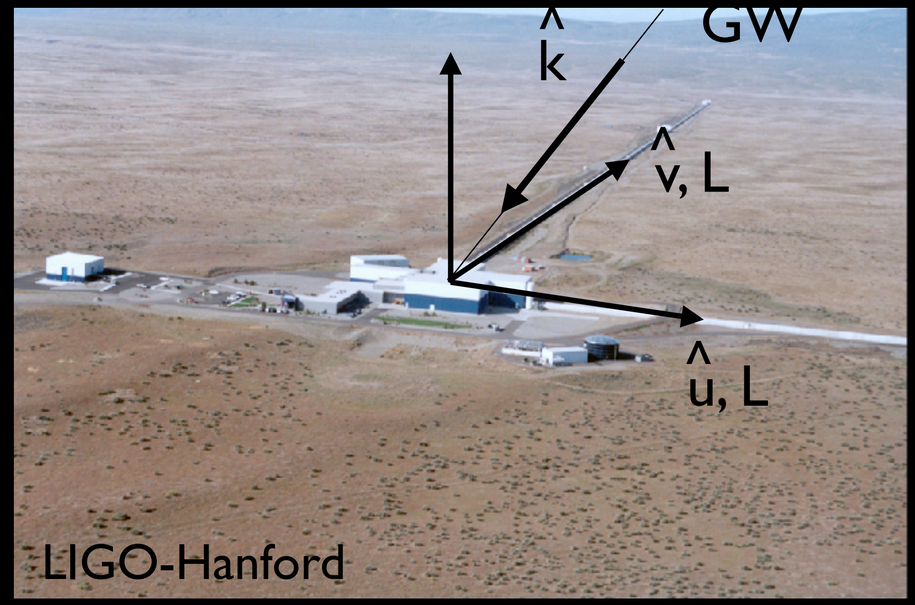

(credit: J. Romano)

$$R^A(f,\hat{n}) \simeq \frac{1}{2}\left(u^a u^b - v^a v^b\right)\, e^A_{ab}(\hat{n})$$

BEAM PATTERN FUNCTIONS

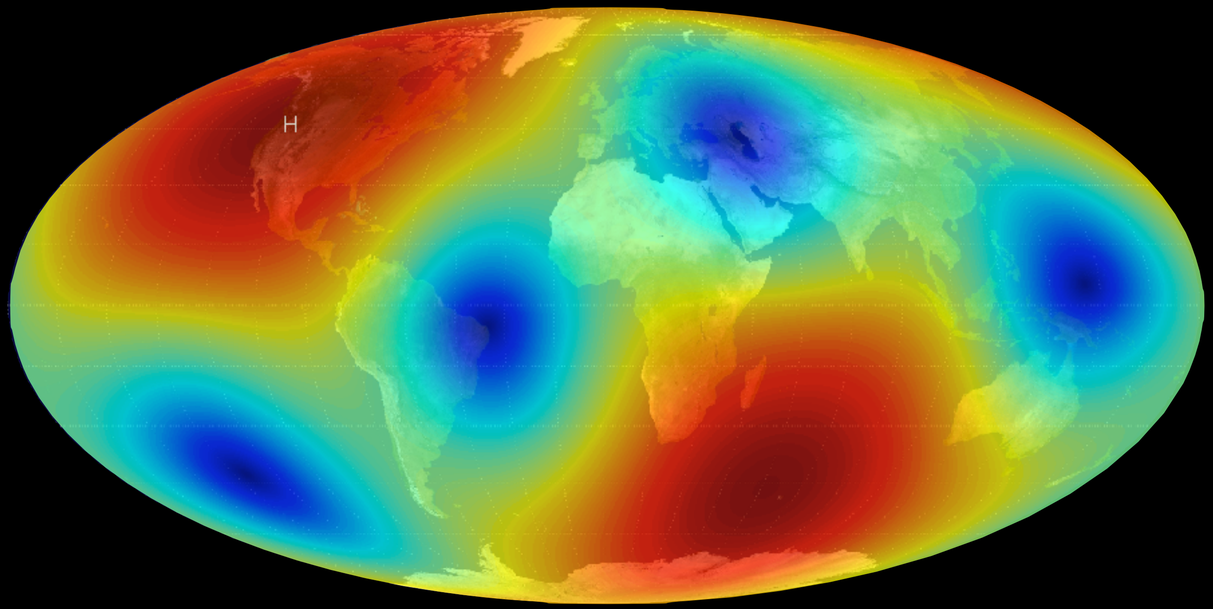

(credit: N. Cornish)

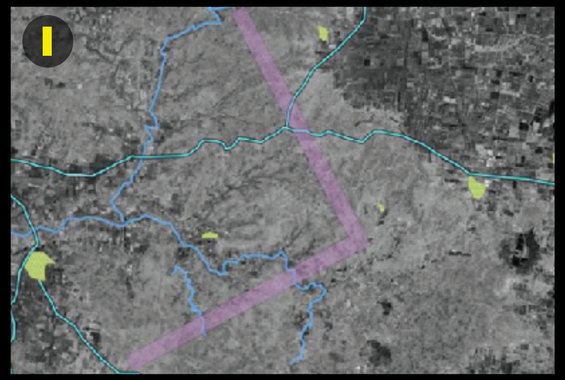

BEAM PATTERN FUNCTIONS

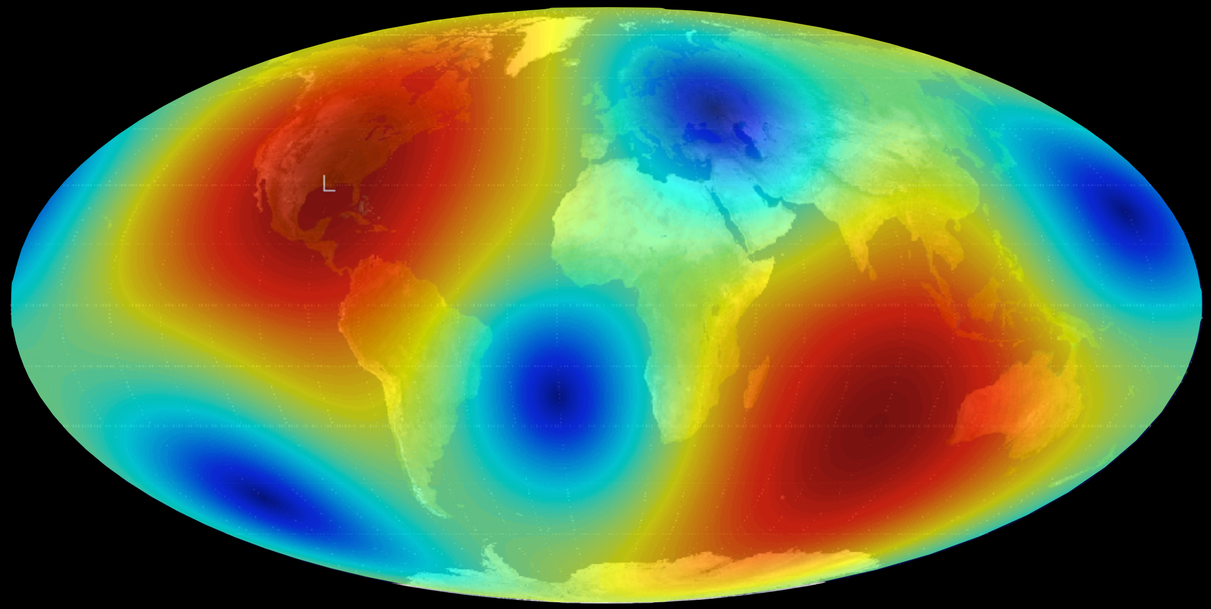

(credit: N. Cornish)

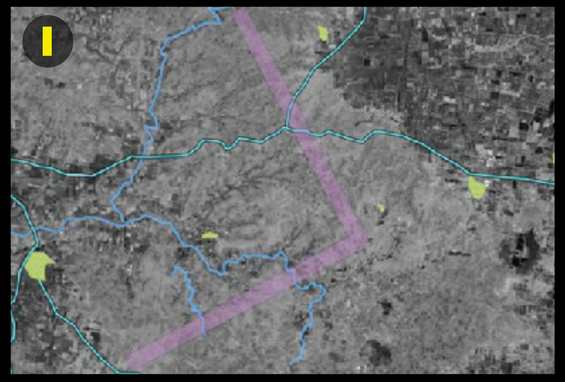

BEAM PATTERN FUNCTIONS

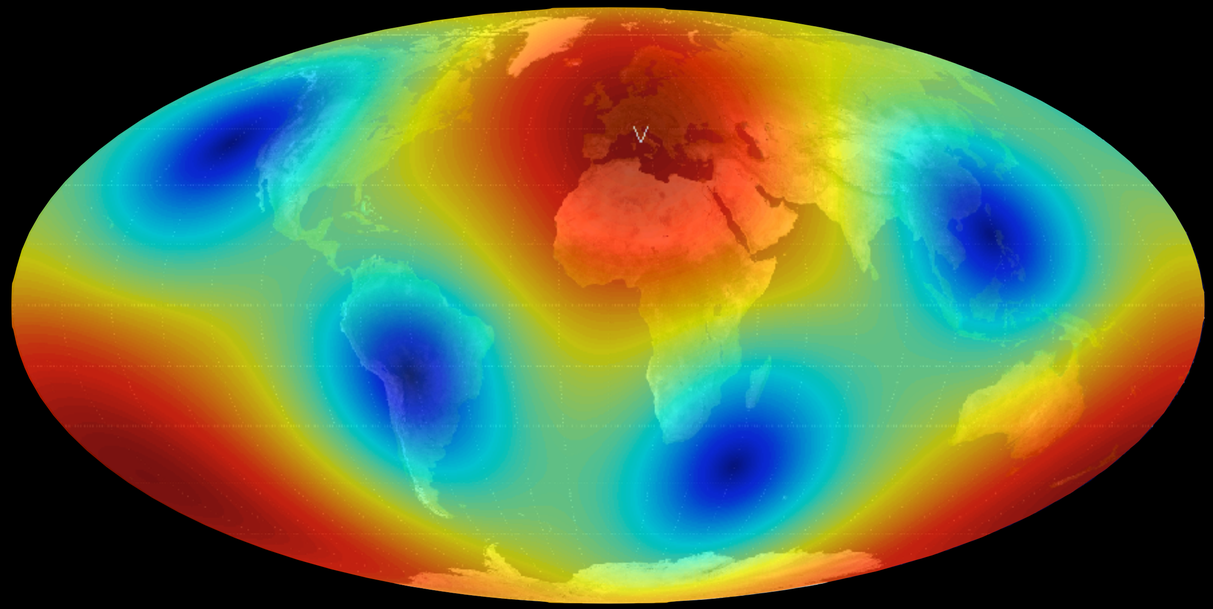

(credit: N. Cornish)

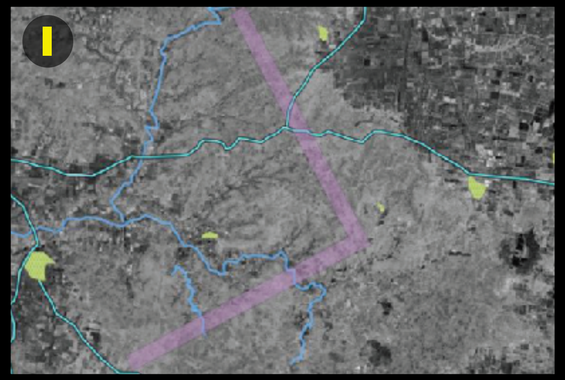

BEAM PATTERN FUNCTIONS

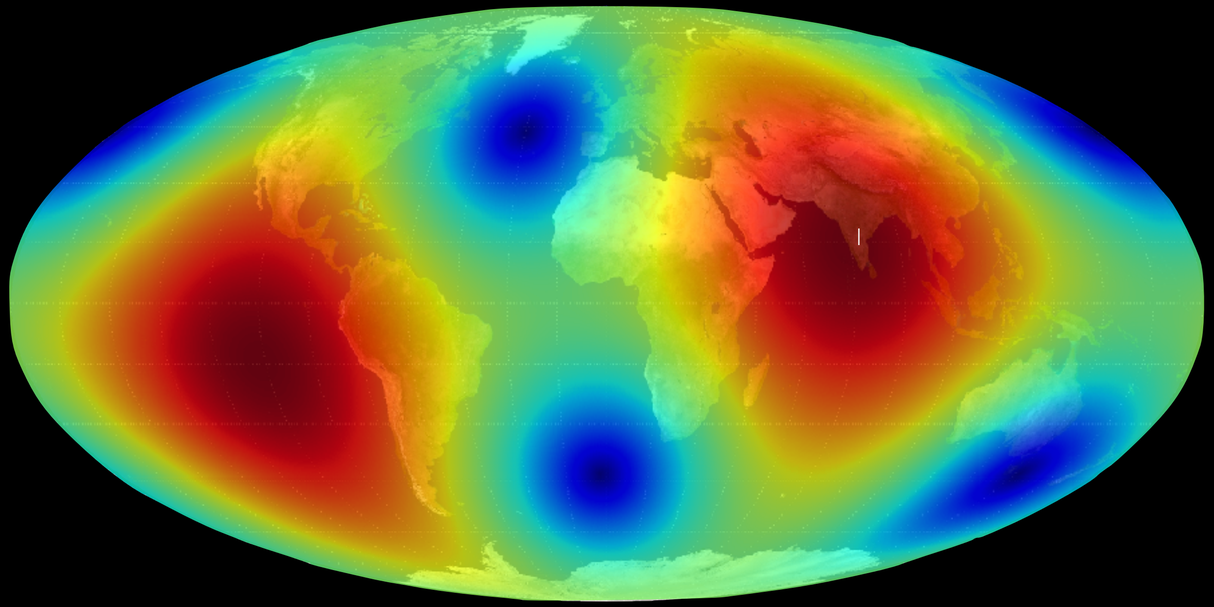

(credit: N. Cornish)

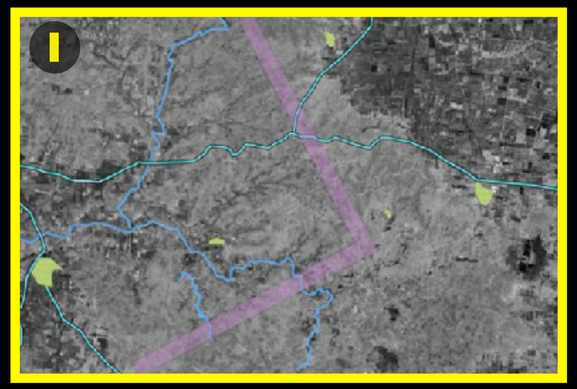

BEAM PATTERN FUNCTIONS

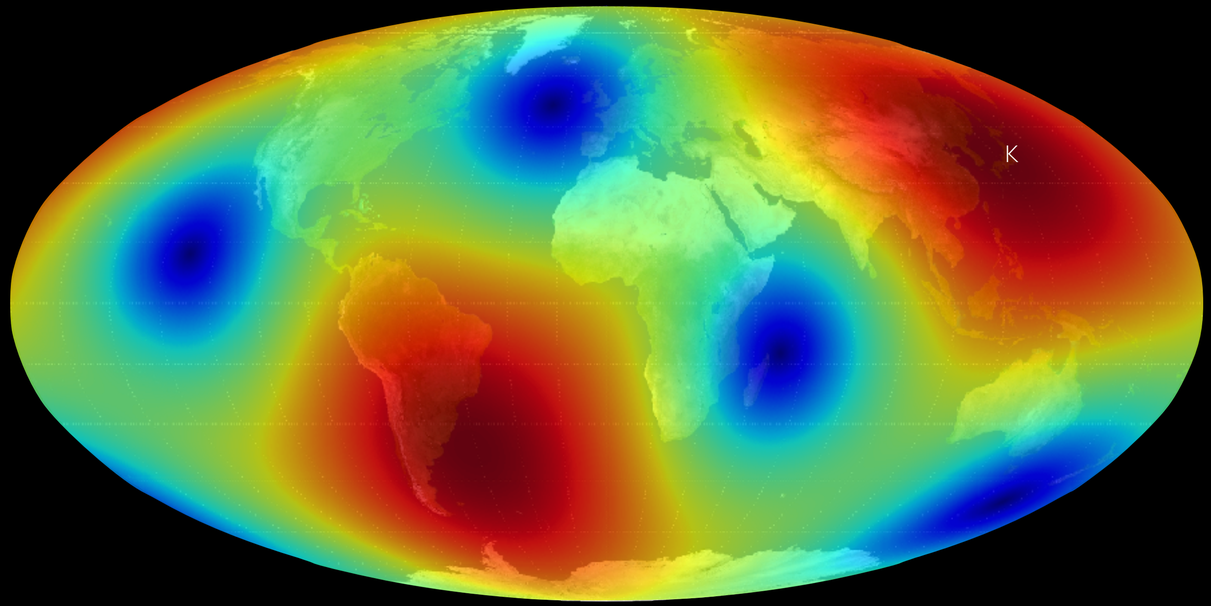

(credit: N. Cornish)

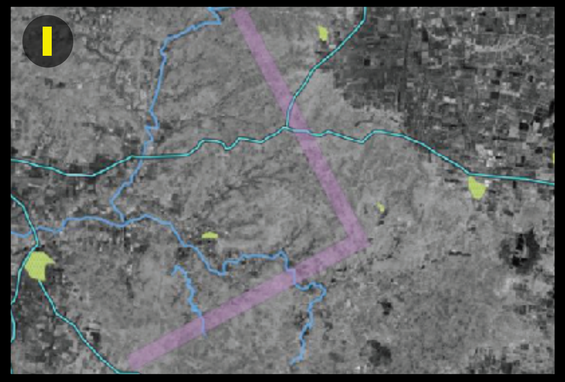

STOCHASTIC GRAVITATIONAL WAVE BACKGROUND

Overlap function (correlation coefficient)

- Detectors in different locations and with different orientations respond differently to a passing GW.
- Overlap function encodes reduction in sensitivity of a cross-correlation analysis due to separation and misalignment of the detectors.

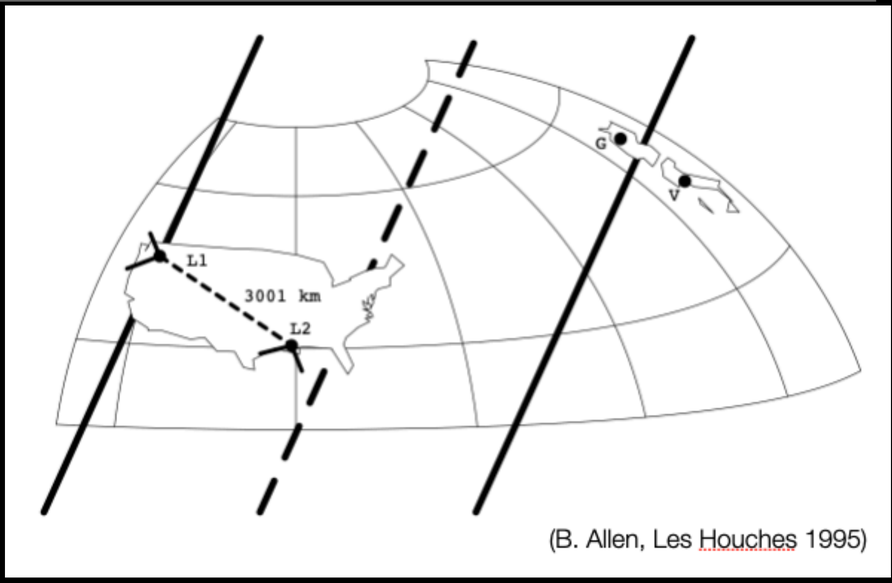

(B. Allen, Les Houches 1995)

Expected correlation:

$$\langle h_I(t) h_J(t') \rangle = \frac{1}{2} \int_{-\infty}^{\infty} \mathrm{d}f \, e^{i2\pi f(t-t')} \Gamma_{IJ}(f) S_h(f) \iff \langle \tilde{h}_I(f) \tilde{h}_J^*(f') \rangle = \frac{1}{2} \delta(f-f') \Gamma_{IJ}(f) S_h(f)$$

$$\Gamma_{IJ}(f) = \frac{1}{8\pi} \sum_A F^A_{\mathcal{I}_1}(\hat{\mathbf{n}}_p, t) \, F^A_{\mathcal{I}_2}(\hat{\mathbf{n}}_p, t) \, e^{2\pi i f \, \hat{\mathbf{n}}_p \cdot \mathbf{\Delta x}_{\mathcal{I}}(t)/c}$$

(unpolarized, stationary, isotropic background)

$\Gamma_{IJ}(f)$ is the transfer function between GW power and detector cross-power;
integrand of $\Gamma_{IJ}(f)$ is important for anisotropic stochastic backgrounds

STOCHASTIC GRAVITATIONAL WAVE BACKGROUND

Overlap function for Hanford-Livingston baseline (correlation coefficient)

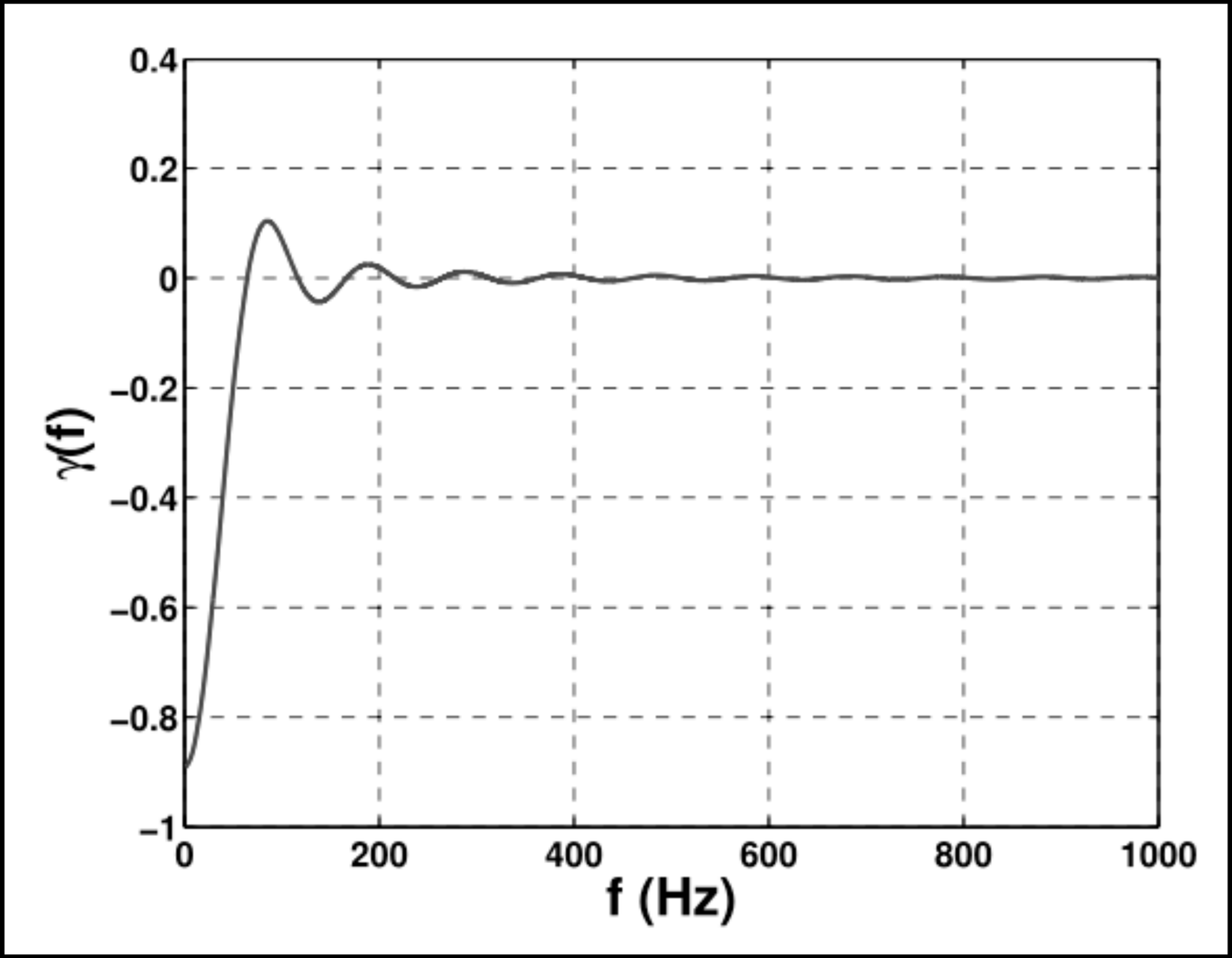

Negative values —> Detectors are rotated 90 degree relative the other.

Not -1 —> Two interferometers are not in the same plane.

Zeros—> At specific frequencies, we have no sensitivity to the gravitational waves

DETECTION STRATEGY

What is the optimal way to correlate data from two physically separated and possibly misaligned detectors to search for a GWB

Cross-correlation estimators / optimal filtering

Cross-correlation estimator $$\hat{S}_h \simeq \int_{-\infty}^{\infty} \mathrm{d}f \int_{-\infty}^{\infty} \mathrm{d}f'\, \delta_T(f-f')\, \tilde{d}_1(f)\, \tilde{d}_2^*(f')\, \tilde{Q}^*(f')$$

Variance $$\sigma^2 \simeq \frac{T}{2} \int_0^{\infty} \mathrm{d}f\, P_1(f)\, P_2(f)\, |\tilde{Q}(f)|^2$$

What we mean by optimal:

Choose Q to maximize SNR for fixed spectral shape:

$$\tilde{Q}(f) \propto \frac{\Gamma_{12}(f)\, H(f)}{P_1(f)\, P_2(f)}$$

expected signal spectrum

de-weight correlation when noise is large or overlap is small

correlation coeff (overlap) between two detectors

DETECTION STRATEGIES FOR THE ISOTROPIC SGWB

PRD104, 022004 (2021)

The observed cross-correlation spectra combining data from all three baselines in O3, as well as the HL baseline in O1 and O2. The spectrum is consistent with expectations from uncorrelated, Gaussian noise.

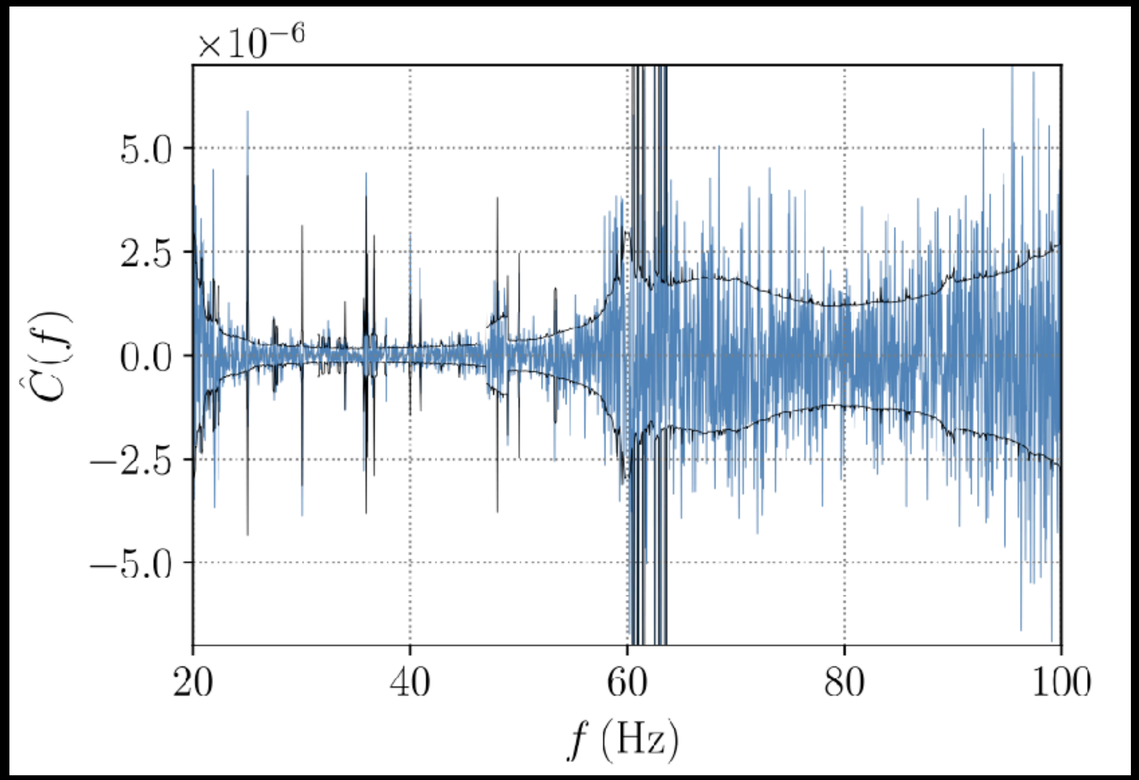

Place upper limits on Ω_α for different power-law indices α.

Upper limits on Ω_α

α	O3	O2 [44]	Improvement
0	5.8×10^{-9}	3.5×10^{-8}	6.0
2/3	3.4×10^{-9}	3.0×10^{-8}	8.8
3	3.9×10^{-10}	5.1×10^{-9}	13.1

DETECTION STRATEGIES FOR THE ISOTROPIC SGWB

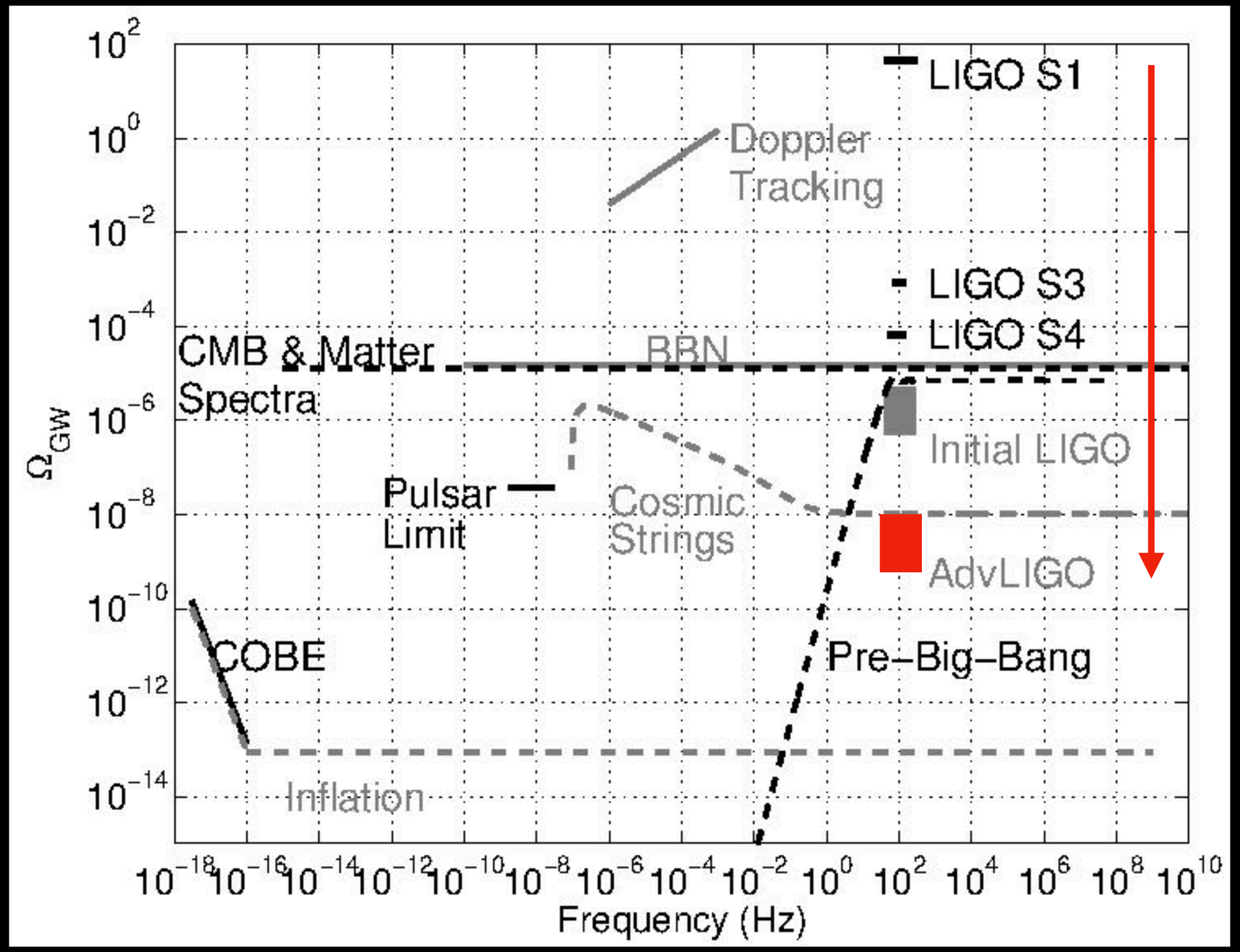

[LIGO S4 - APJ 659:918, 2007]

Improvement in upper limits over the last two decades

We are on the right track!!

TYPES OF STOCHASTIC GRAVITATIONAL WAVE BACKGROUND

(i) Stochastic backgrounds can differ in spatial distribution

(statistically) isotropic

There may be inhomogeneities in the GW source mechanisms, for example a particular distribution of the sources on the sky, which produces an anisotropic signal.

As gravitational-wave propagate, they accumulate line-of-sight effects, crossing different matter density fields which are inhomogeneously distributed in the Universe.

(like cosmic microwave background)

anisotropic

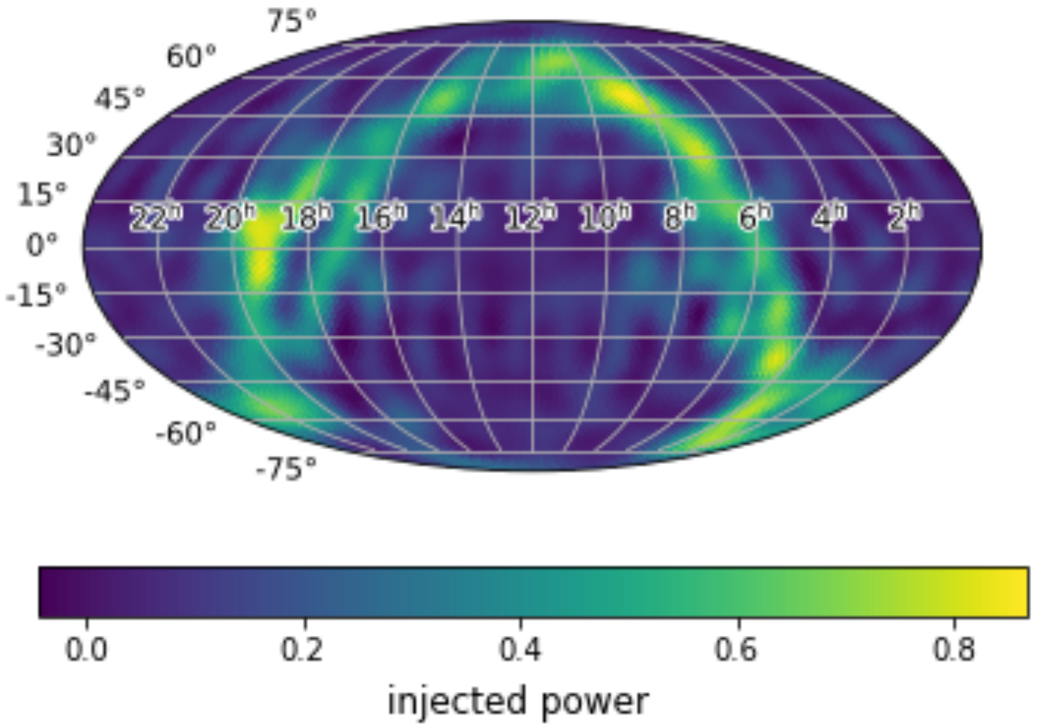

(galactic plane in equatorial coords)

Cross-Correlation is essentially a one dimensional map of the sky

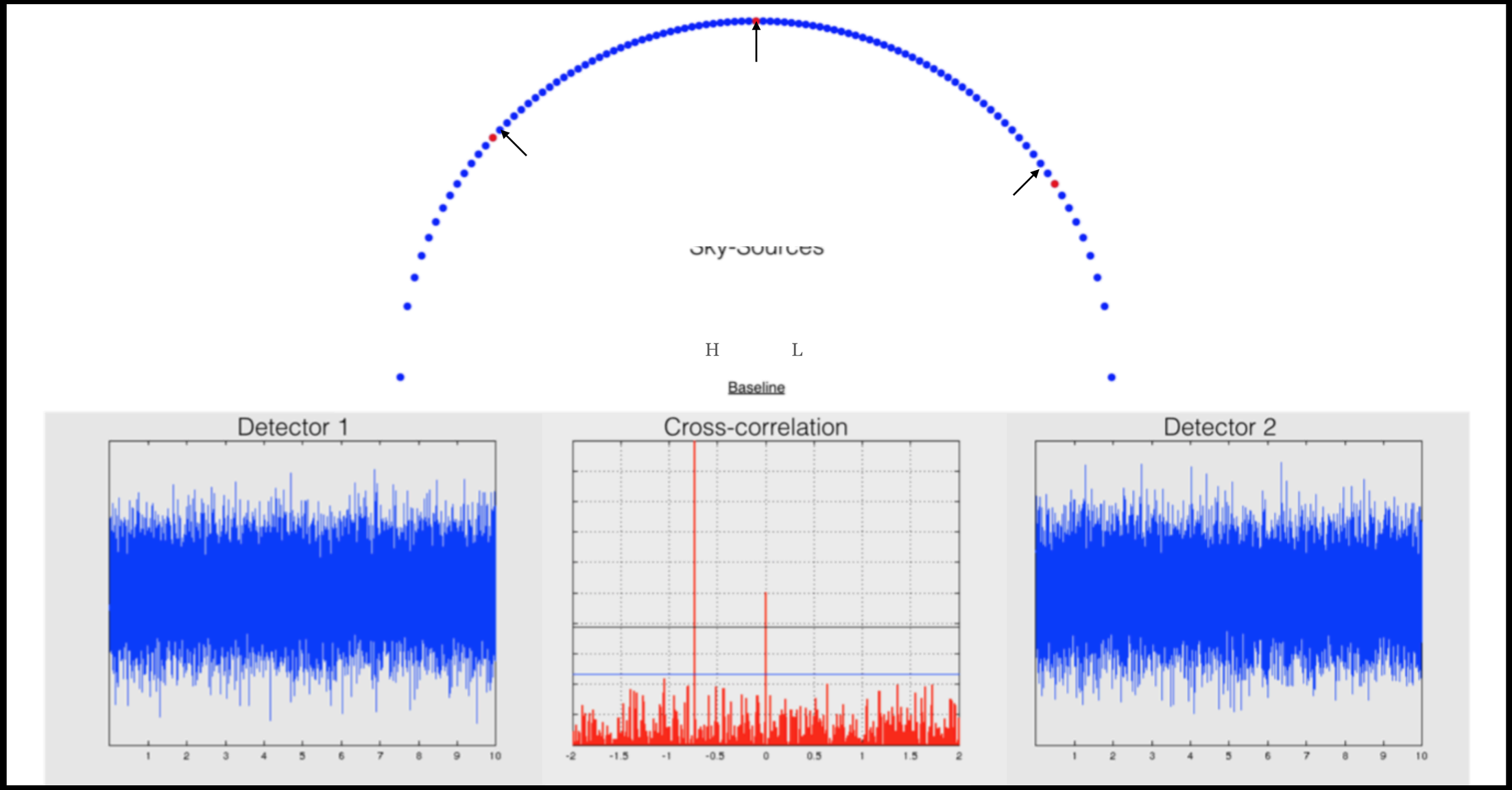

Base Line Sidereal Rotation

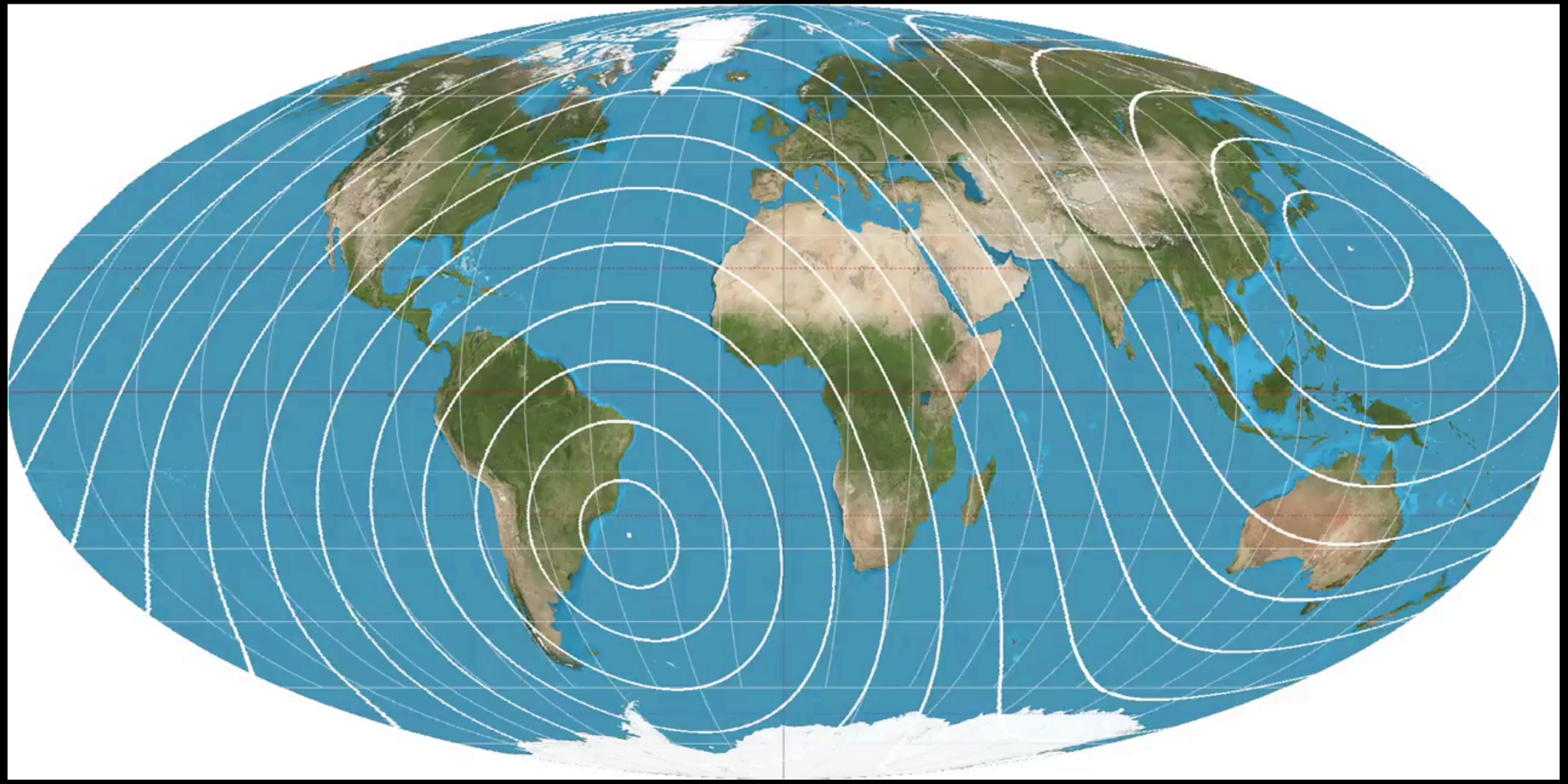

The white circles indicate positions in the sky map that will have equal time/phase delay when the signal from that part of the sky arrives in the LIGO Livingston and Hanford detectors.

Pre-Processing

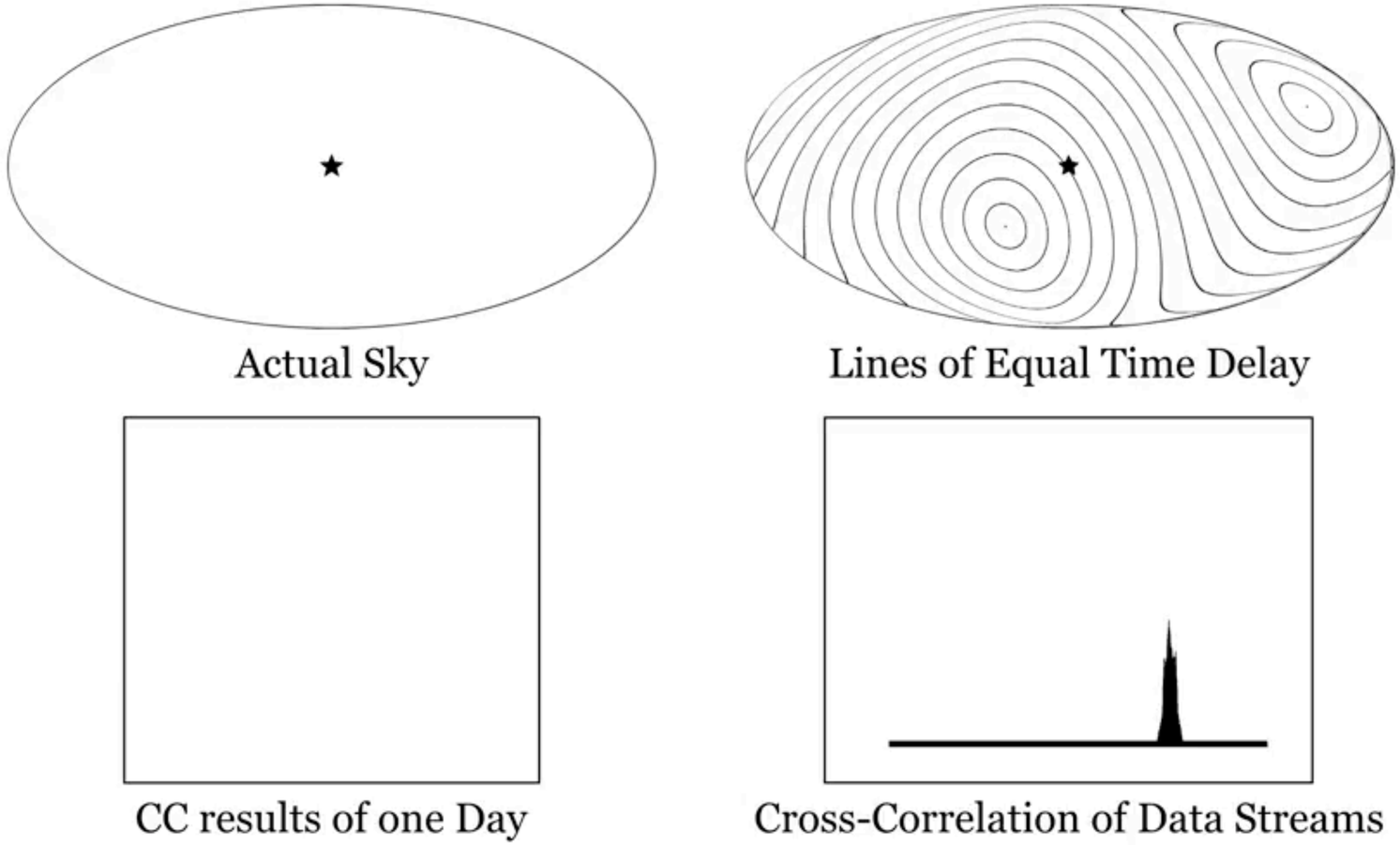

For a point source in sky (top-left) the cross-correlation results are calculated (bottom right) and stored (bottom left).

Credit: A. Ain

What happens in real-life

1. Split the data taken from the detectors (time-series data) into chunks of duration
2. Data quality cuts are applied
3. Cross-correlate the time series from a detector baseline.
4. Consider the ORF

Processing

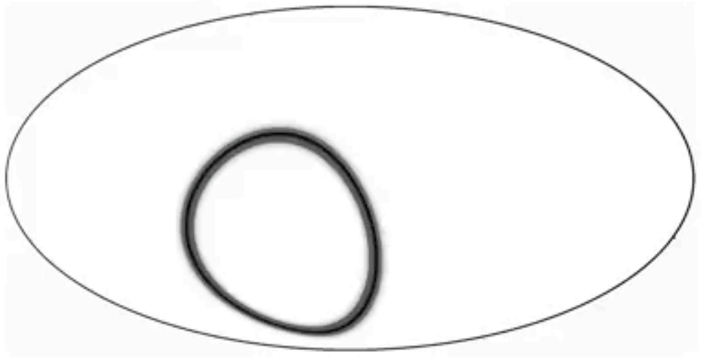

Map from CC results

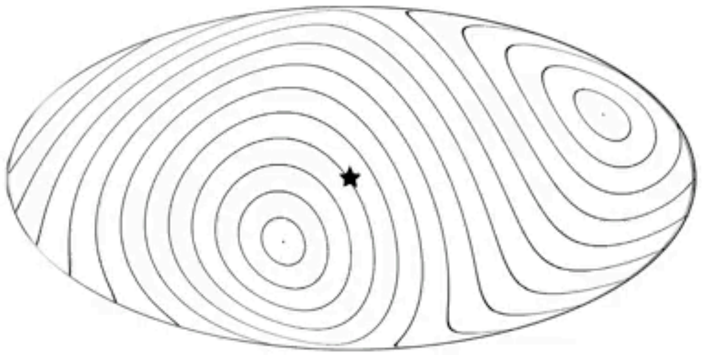

Lines of Equal Time Delay

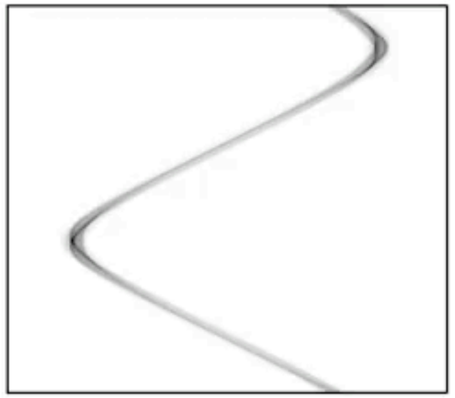

CC results of one Day

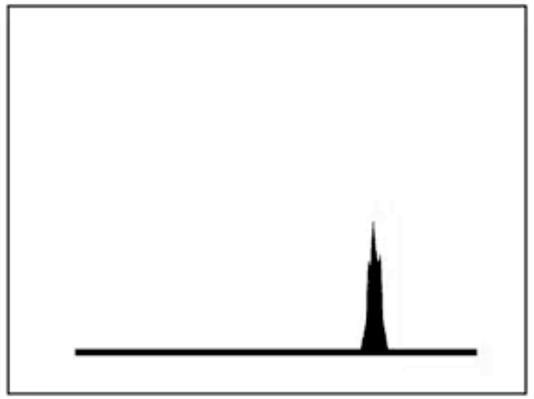

Cross-Correlation of Data Streams

For a point source in sky the cross-correlation results are turned into maps (top-left).

What happens in real-life

1. Split the data taken from the detectors (time-series data) into chunks of duration
2. Data quality cuts are applied
3. Cross-correlate the time series from a detector baseline.
4. Consider the ORF

Credit: A. Ain

Post-Processing

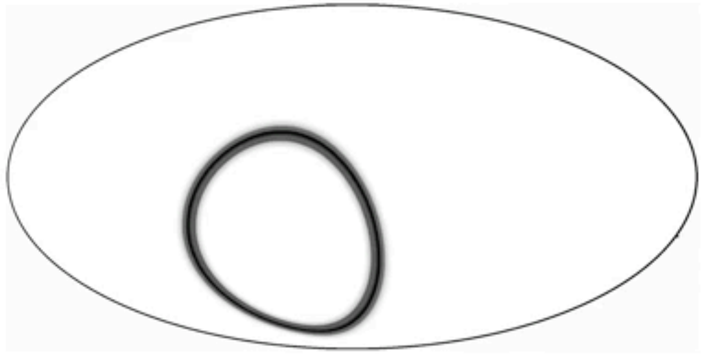

Map from CC results

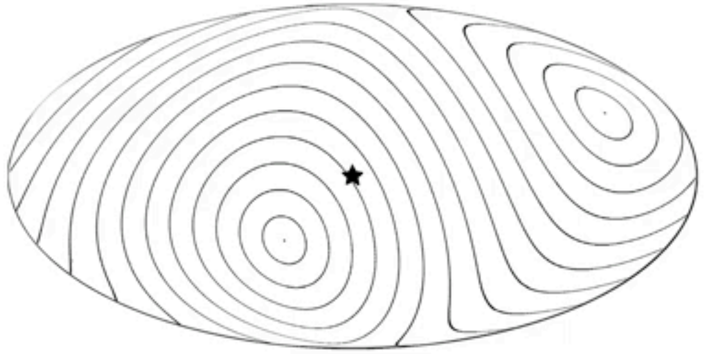

Lines of Equal Time Delay

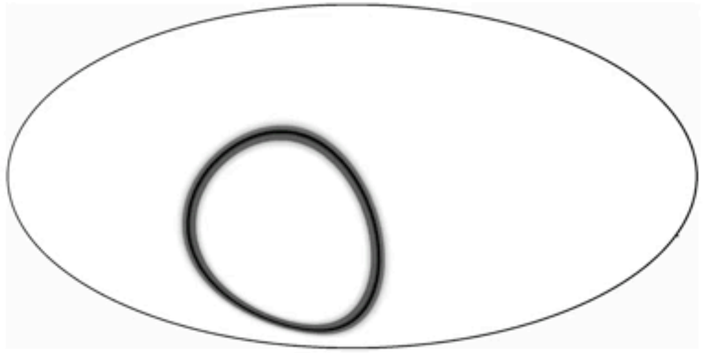

Sum of all CC Map results

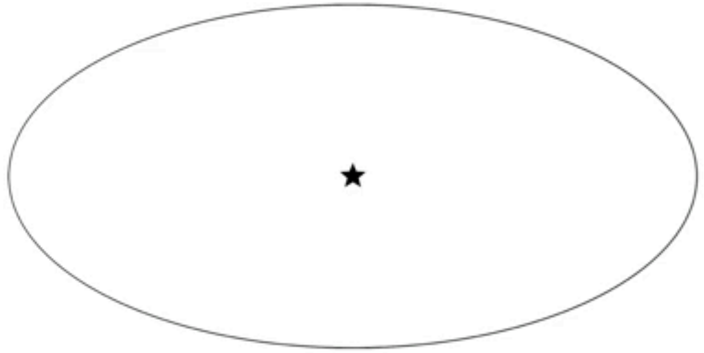

Actual Sky

For a point source in sky the maps from all segments (top-left) are cumulatively added (bottom-left).

What happens in real-life

1. Split the data taken from the detectors (time-series data) into chunks of duration
2. Data quality cuts are applied
3. Cross-correlate the time series from a detector baseline.
4. Consider the ORF

Credit: A. Ain

RADIOMETER ALGORITHM

The anisotropy of the SGWB can be characterized using the dimensional energy density parameter

$$\Omega_{\mathrm{GW}}(f,\hat{\mathbf{n}}) \equiv \frac{f}{\rho_c}\frac{d\rho_{\mathrm{GW}}}{df} = \frac{2\pi^2}{3H_0^2} f^3 \mathscr{P}(f,\hat{\mathbf{n}})$$

- Essentially Earth Rotation Synthesis Imaging
  - cross-correlate detector outputs in short-time segments
  - map making: use time-dependent phase delay
- Use spectral filters
  - to enhance signal power
  - to reduce noise power

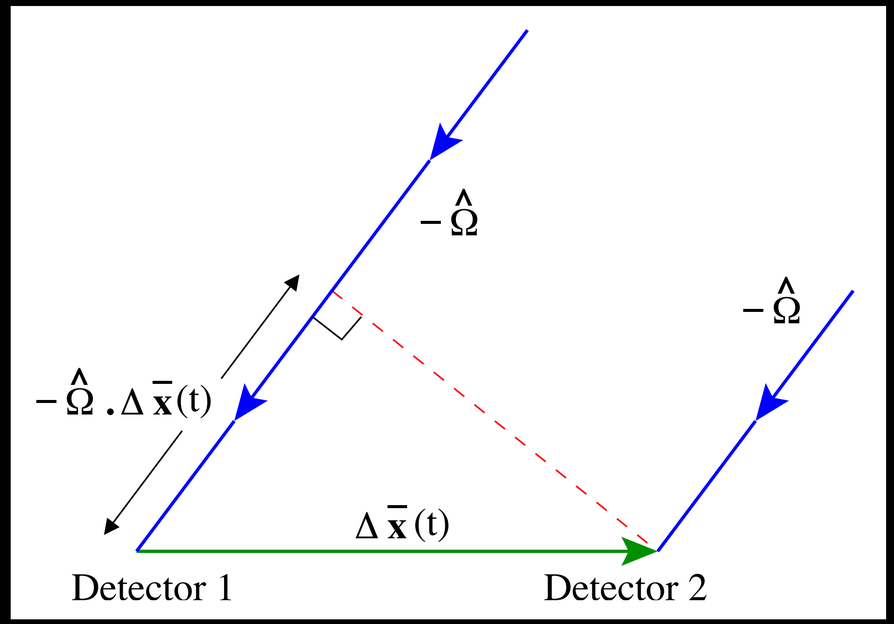

Lazzarini+2004 Ballmer+2006 Mitra+2007

Here $\Delta x(t)$ is the separation or baseline vector between the two detectors; as the Earth rotates, its direction changes, but its magnitude remains fixed. The direction to the source $\hat{\Omega}$ is also fixed in the barycentric frame. The phase difference between signals arriving at two detector sites from the same direction is also shown.

RADIOMETER ALGORITHM

The anisotropy of the SGWB can be characterized using the dimensional energy density parameter

$$\Omega_{\mathrm{GW}}(f,\hat{\mathbf{n}}) \equiv \frac{f}{\rho_c}\frac{d\rho_{\mathrm{GW}}}{df} = \frac{2\pi^2}{3H_0^2} f^3 \mathscr{P}(f,\hat{\mathbf{n}})$$

- Essentially Earth Rotation Synthesis Imaging
  - cross-correlate detector outputs in short-time segments
  - map making: use time-dependent phase delay
- Use spectral filters
  - to enhance signal power
  - to reduce noise power

Most of the analysis performed so far assumes that the frequency and direction dependiecs can be separated:

$$\mathscr{P}(f,\hat{\mathbf{n}}) = P(\hat{\mathbf{n}})\, H(f)$$

Lazzarini+2004 Ballmer+2006 Mitra+2007

Here $\Delta x(t)$ is the separation or baseline vector between the detector sites; its direction changes, but its magnitude remains fixed. The direction to the source $\hat{\Omega}$ is also fixed in the barycentric frame. The phase difference between signals arriving at two detector sites from the same direction is also shown.

Where the common choice of spectral shape is $H(f) = \left(\frac{f}{f_{\mathrm{ref}}}\right)^{\beta}$

RADIOMETER ALGORITHM

The anisotropy of the SGWB can be characterized using the dimensional energy density parameter

$$\Omega_{\mathrm{GW}}(f,\hat{\mathbf{n}}) \equiv \frac{f}{\rho_c}\frac{d\rho_{\mathrm{GW}}}{df} = \frac{2\pi^2}{3H_0^2} f^3 \mathscr{P}(f,\hat{\mathbf{n}})$$

- Essentially Earth Rotation Synthesis Imaging
  - cross-correlate detector outputs in short-time segments
  - map making: use time-dependent phase delay
- Use spectral filters
  - to enhance signal power
  - to reduce noise power

Most of the analysis performed so far assumes that the frequency and direction dependiecs can be separated:

Where the conventional choice of spectral shape is $H(f) = \left(\frac{f}{f_{\mathrm{ref}}}\right)^{\beta}$

Lazzarini+2004 Ballmer+2006 Mitra+2007

Here $\Delta x(t)$ is the separation or baseline vector between the detector sites; its direction changes, but its magnitude remains fixed. The direction to the source $\hat{\Omega}$ is also fixed in the barycentric frame. The phase difference between signals arriving at two detector sites from the same direction is also shown.

We will perform a model-independent search

RADIOMETER SEARCH

Observed data:

$$C^I \equiv C^I_{ft} = \tilde{s}^*_1(t,f)\,\tilde{s}_2(t,f)$$

Noise (in the weak signal limit):

$$n^I \equiv n^I_{ft} = \tilde{n}^*_1(t,f)\,\tilde{n}_2(t,f)$$

Covariance matrix:

$$\mathcal{N}_{ft,f't'} = \mathsf{Cov}(C^I_{ft}, C^{I'}_{f't'}) \approx \frac{(\Delta T)^2}{4}\,\delta_{II'}\,\delta_{tt'}\,\delta_{ff'}\,P_2(t,f)\,P_1(t,f)$$

RADIOMETER SEARCH

To estimate the anisotropy of the SGWB, one can set up a likelihood function and then attempt to maximize it.

$$\mathscr{L} \propto \exp\left[-(C^{*}_{ft} - < C^{*}_{ft} >)\, \mathscr{N}^{-1}_{ft,f't'}\, (C_{f't'} - < C_{f't'} >)\right]$$

The maximum likelihood (ML) estimator of the SGWB anisotropy in the presence of additive Gaussian noise is then given by

$$\hat{\mathscr{P}} = \mathbf{\Gamma}^{-1}\, \mathbf{X}$$

Dirty Map —> Map of the SGWB convolved with the detector's response.

Clean Map —> Response of the detectors are deconvolved

Fisher Matrix —> Covariance matrix of the dirty map.

RADIOMETER SEARCH

The “narrowband dirty map” is given as

$$X_p(f) \;=\; \sum_{\mathcal{J}t} \frac{\gamma^{\mathcal{J}*}_{ft,p}\, C^{\mathcal{J}}(t;f)}{P_{\mathcal{J}_1}(t;f) P_{\mathcal{J}_2}(t;f)}\,,$$

Cross Spectral Density $\langle C^{\mathcal{J}}(t;f)\rangle \propto \hat{\mathscr{P}}(f,\hat{\mathbf{n}}_p)\,\gamma^{\mathcal{J}}_{ft,p}$

The noise covariance matrix in a weak signal limit is given by

$$\Gamma_{pp'}(f) \;=\; \sum_{\mathcal{J}t} \frac{\gamma^{\mathcal{J}*}_{ft,p}\,\gamma^{\mathcal{J}}_{ft,p'}}{P_{\mathcal{J}_1}(t;f)\,P_{\mathcal{J}_2}(t;f)}\,.$$

Where $\gamma^{\mathcal{J}}_{ft,p}$ is the direction-dependent overlap reduction function,

$$\gamma^{\mathcal{J}}_{ft,p} :\equiv \sum_A F^A_{\mathcal{J}_1}(\hat{\mathbf{n}}_p,t)\,F^A_{\mathcal{J}_2}(\hat{\mathbf{n}}_p,t)\,e^{2\pi i f\,\hat{\mathbf{n}}_p\cdot\Delta\mathbf{x}_{\mathcal{J}}(t)/c}$$

PyStoch: Map-Making Pipeline

A. Ain, J. Suresh & S. Mitra, PRD 98, 024001 (2018)
J. Suresh, A. Ain & S. Mitra, PRD 103, 083024 (2021)

PyStoch : fast HEALPix based SGWB mapmaking

↓

perform the whole analysis on a laptop in a few minutes!

↓

Produces the narrowband maps as an intermediate result

↓

so separate search for different frequency spectra becomes redundant

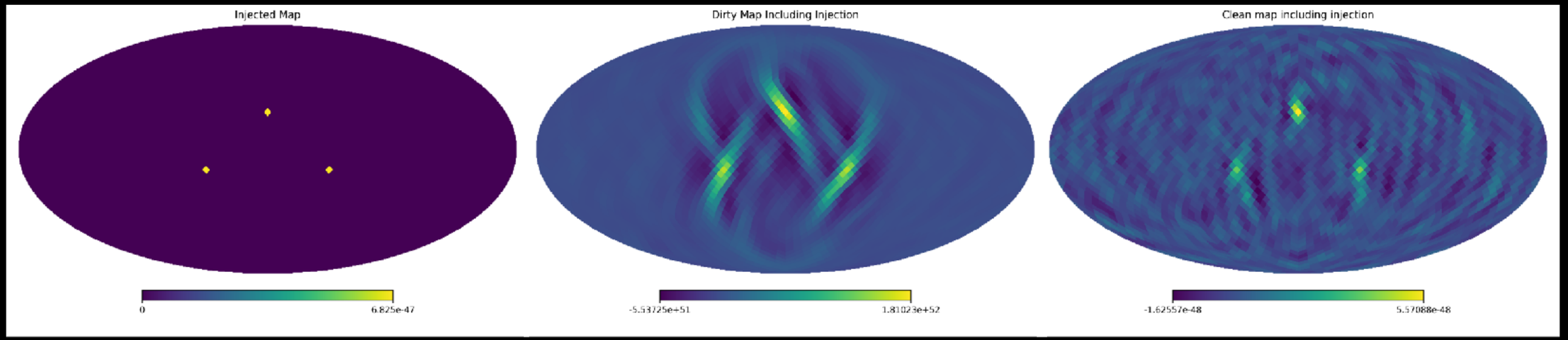

PyStoch: Computing the Overlap Reduction Function

$$\gamma^{\mathcal{I}}_{ft,p} = \sum_A F^A_{\mathcal{I}_1}(\hat{\mathbf{n}}_p, t)\, F^A_{\mathcal{I}_2}(\hat{\mathbf{n}}_p, t)\, e^{2\pi i f\, \hat{\mathbf{n}}_p \cdot \Delta\mathbf{x}_{\mathcal{I}}(t)/c}$$

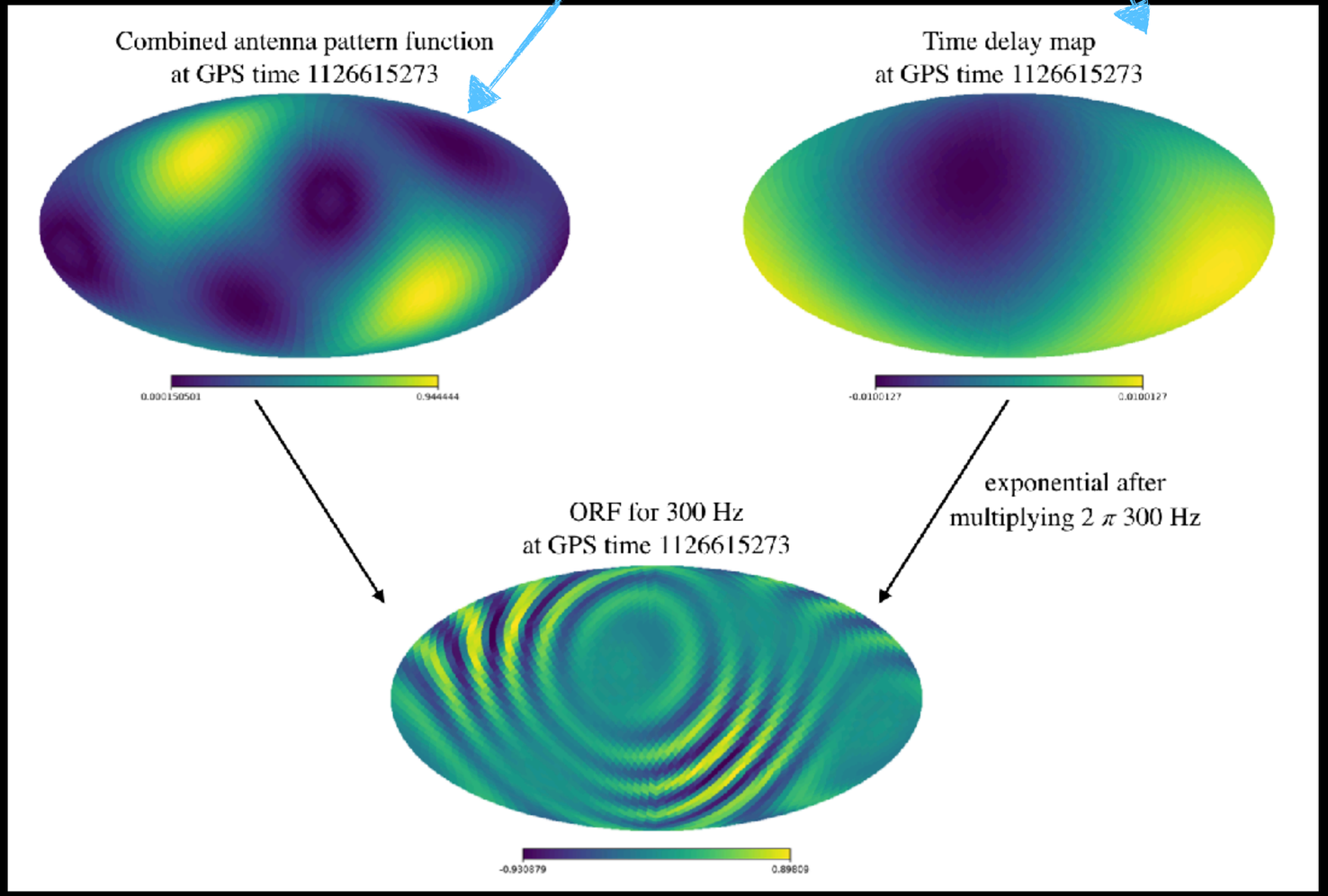

PyStoch: Computing the Overlap Reduction Function

$$\gamma^{\mathcal{I}}_{ft,p} = \sum_{A} F^{A}_{\mathcal{I}_1}(\hat{\mathbf{n}}_p, t)\, F^{A}_{\mathcal{I}_2}(\hat{\mathbf{n}}_p, t)\, e^{2\pi i f\, \hat{\mathbf{n}}_p \cdot \Delta\mathbf{x}_{\mathcal{I}}(t)/c}$$

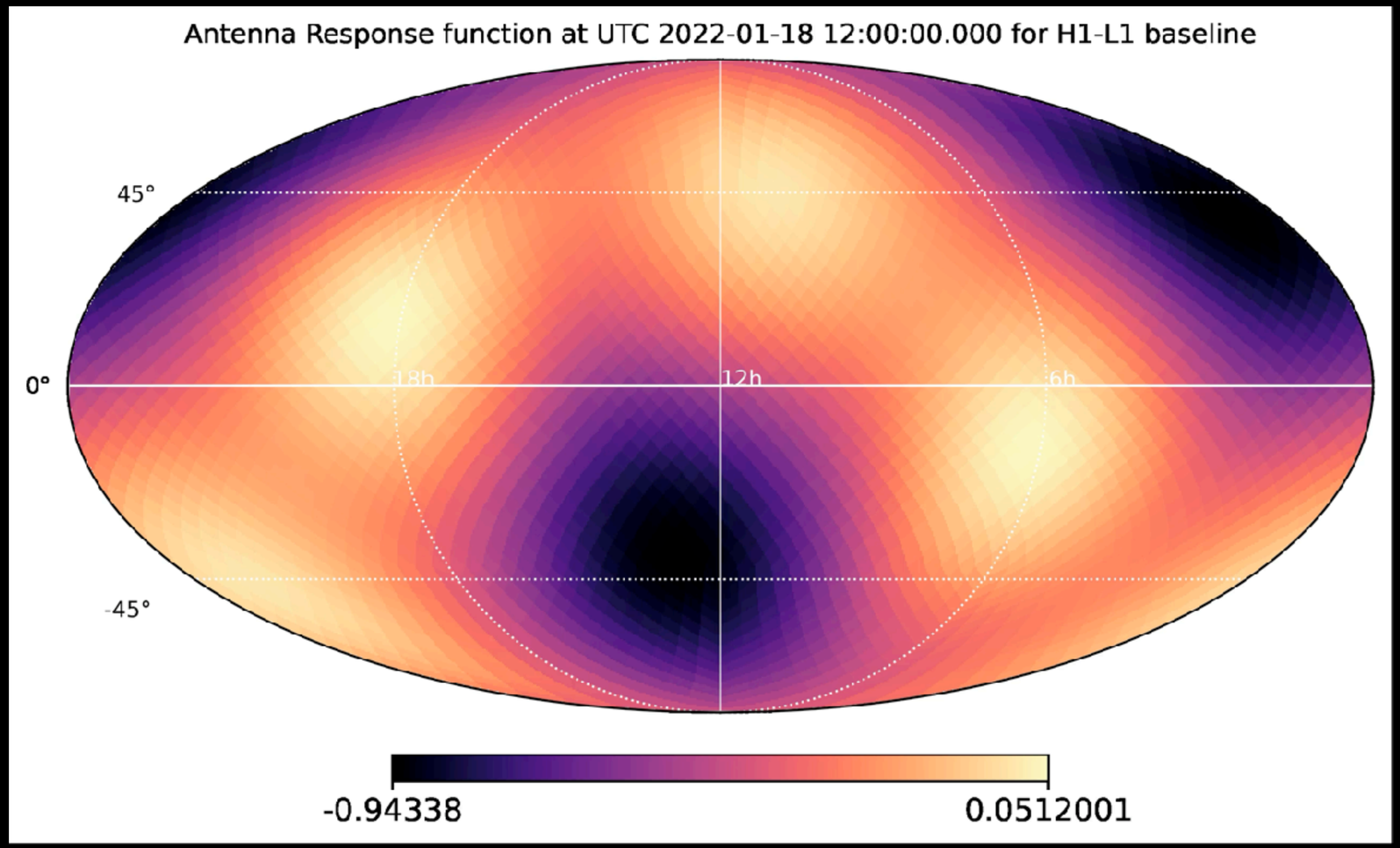

PyStoch: Computing the Overlap Reduction Function

$$\gamma^{\mathcal{J}}_{ft,p} = \sum_{A} F^{A}_{\mathcal{J}_1}(\hat{\mathbf{n}}_p, t)\, F^{A}_{\mathcal{J}_2}(\hat{\mathbf{n}}_p, t)\, e^{2\pi i f\, \hat{\mathbf{n}}_p \cdot \Delta\mathbf{x}_{\mathcal{J}}(t)/c}$$

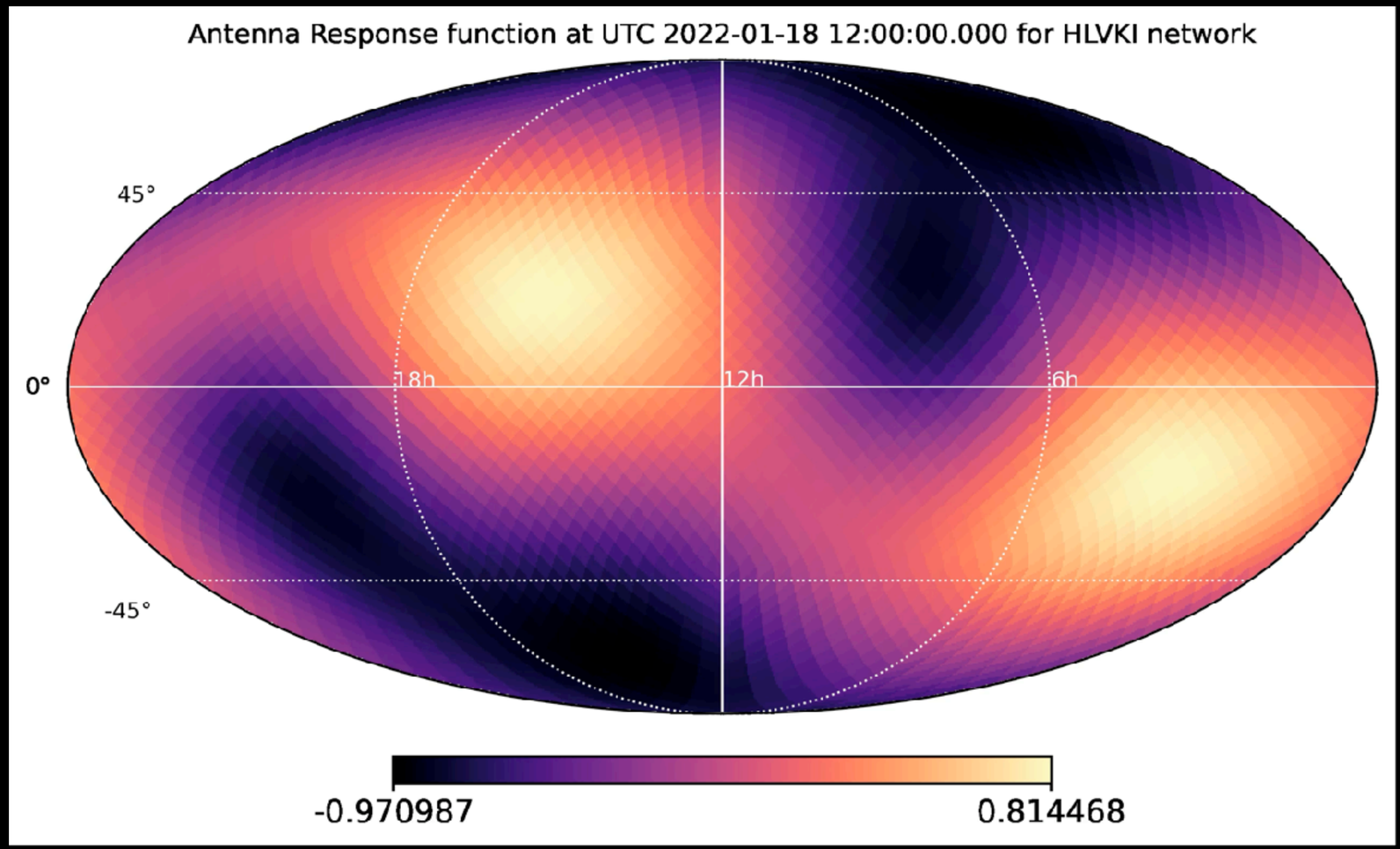

All-Sky All-Frequency Search for SGWB

Now we have all the ingredients to perform an all-sky all-frequency search, which assumes no specific power-law model for the SGWB

Data from LIGO-Virgo-KAGRA's first three observing runs

- Time-series data are sampled at 16384 Hz.
  - Downsample to 4096 Hz, so Nyquist frequency is 2048 Hz.
  - Analyze data below 1726 Hz to avoid aliasing effects.
- The high-pass filter is applied to remove the low-frequency noise (16th-order Butterworth filter, with a knee frequency of 11 Hz)
- Divide data into time segments of duration T=192 s.
  - Hann-windowed and overlapped by 50%.
- Compute discrete Fourier transform on each segment.
- Coarse-grain the spectrum 1/32 Hz.

these data sets will be the input for → PyStoch

All-Sky All-Frequency Search for SGWB

Now we have all the ingredients to perform an all-sky all-frequency search, which assumes no specific power-law model for the SGWB

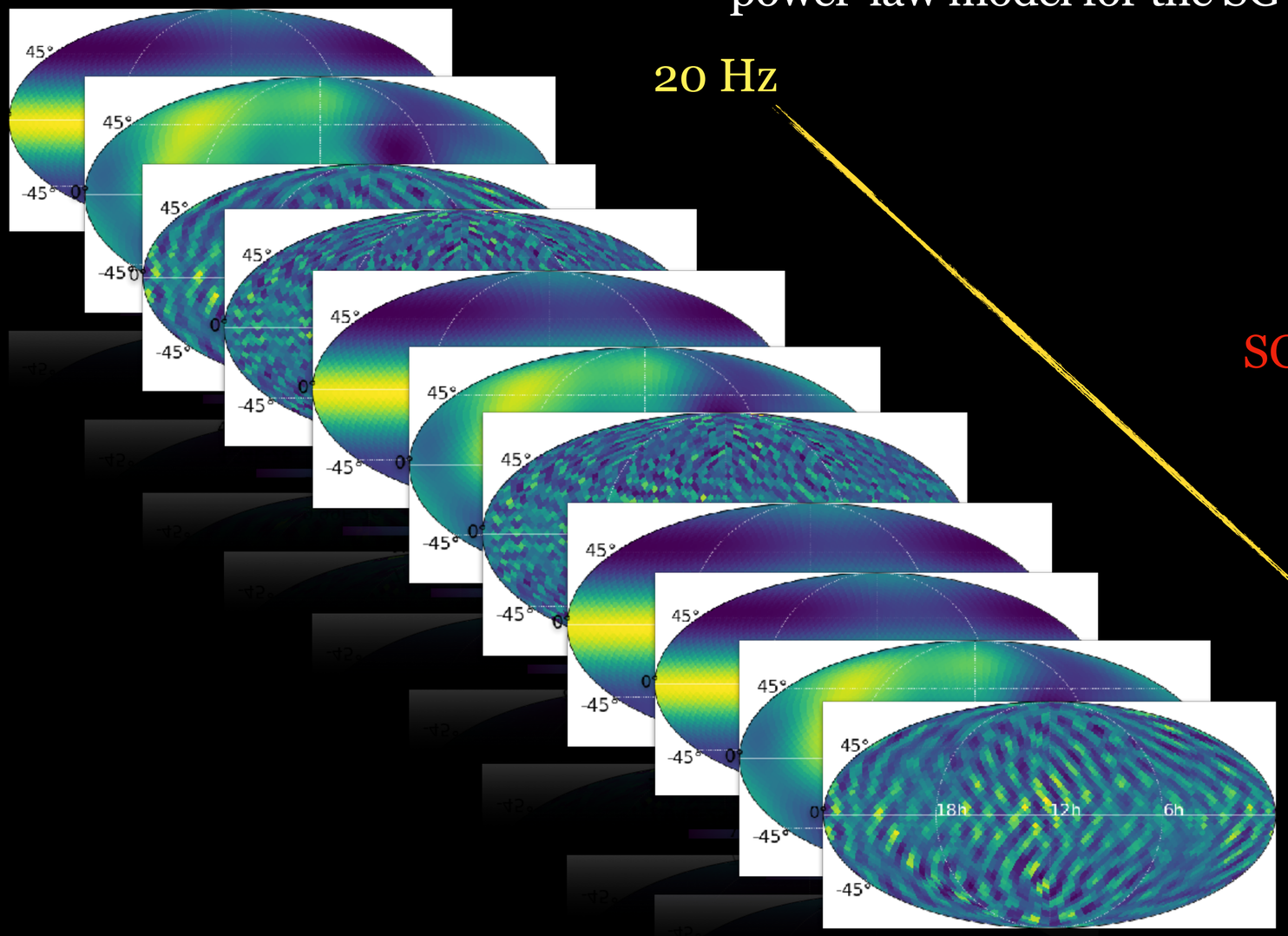

All-Sky All-Frequency Search for SGWB

Injection study to verify the statistics

1. Testing the recovery of the injections performed on the real GW data set

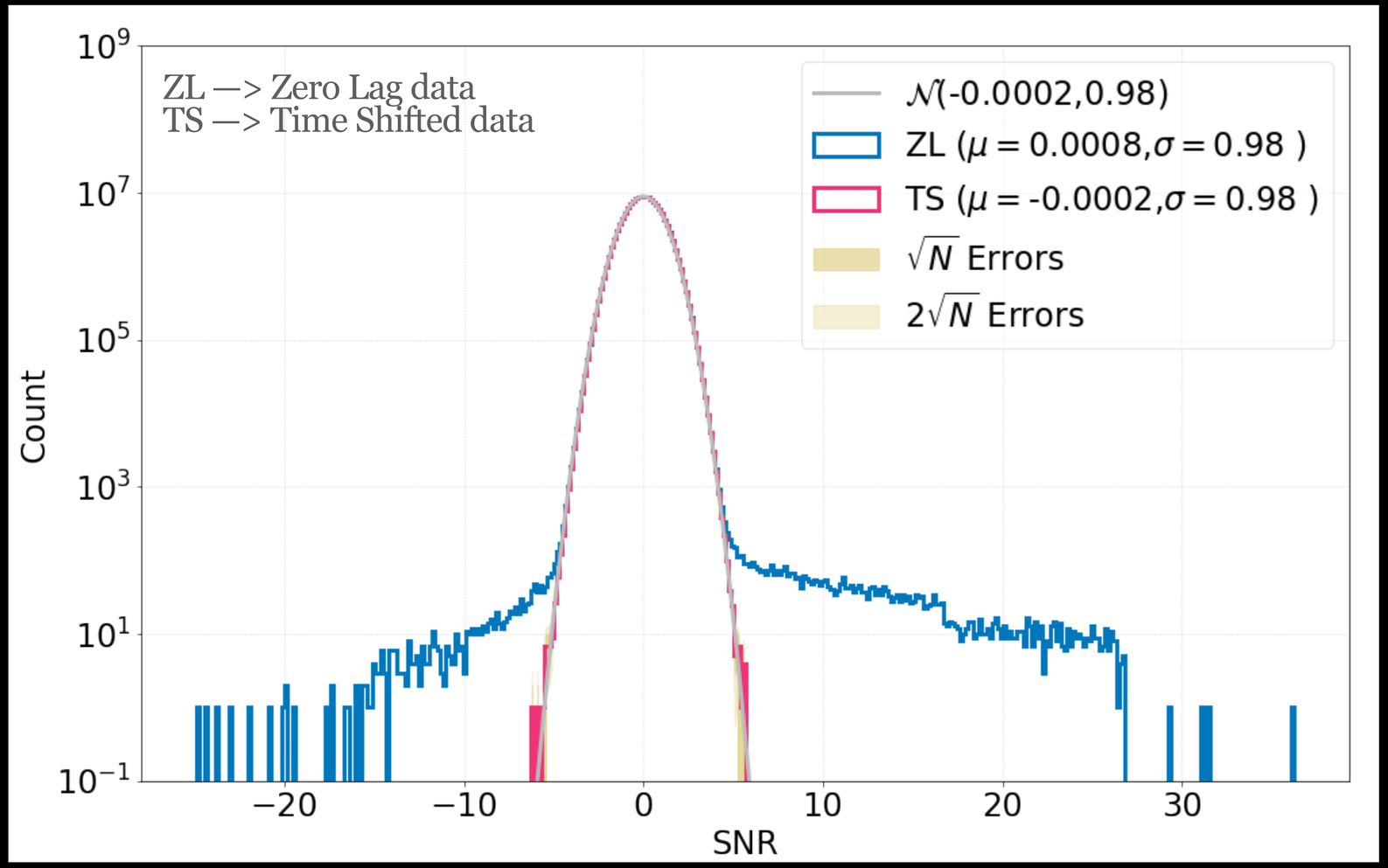

14 monochromatic source injections.

The null distribution is obtained by providing random unphysical time-shift to degrade coherence between two detectors

All-Sky All-Frequency Search for SGWB

Injection study to verify the statistics

1. Maximum SNR distribution and outliers

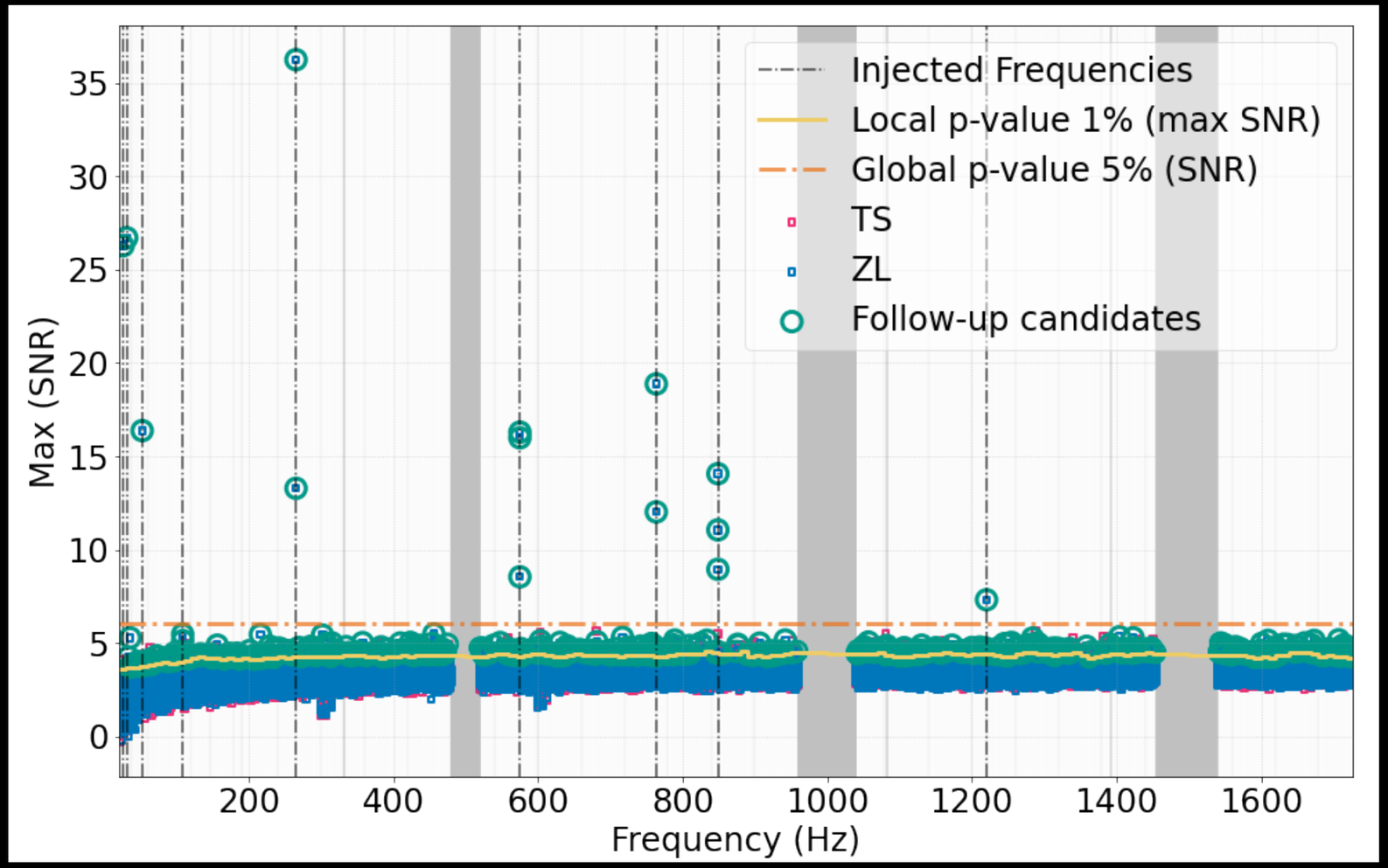

The injections are recovered as an outlier in the nearest frequency bin and the sky location

All-Sky All-Frequency Search for SGWB

R. Abbott et al. (LVK) Phys.Rev.D 105 (2022) 10, 102001

GW data from LIGO-Virgo-KAGRA's first three observing runs (O1 + O2 + O3)

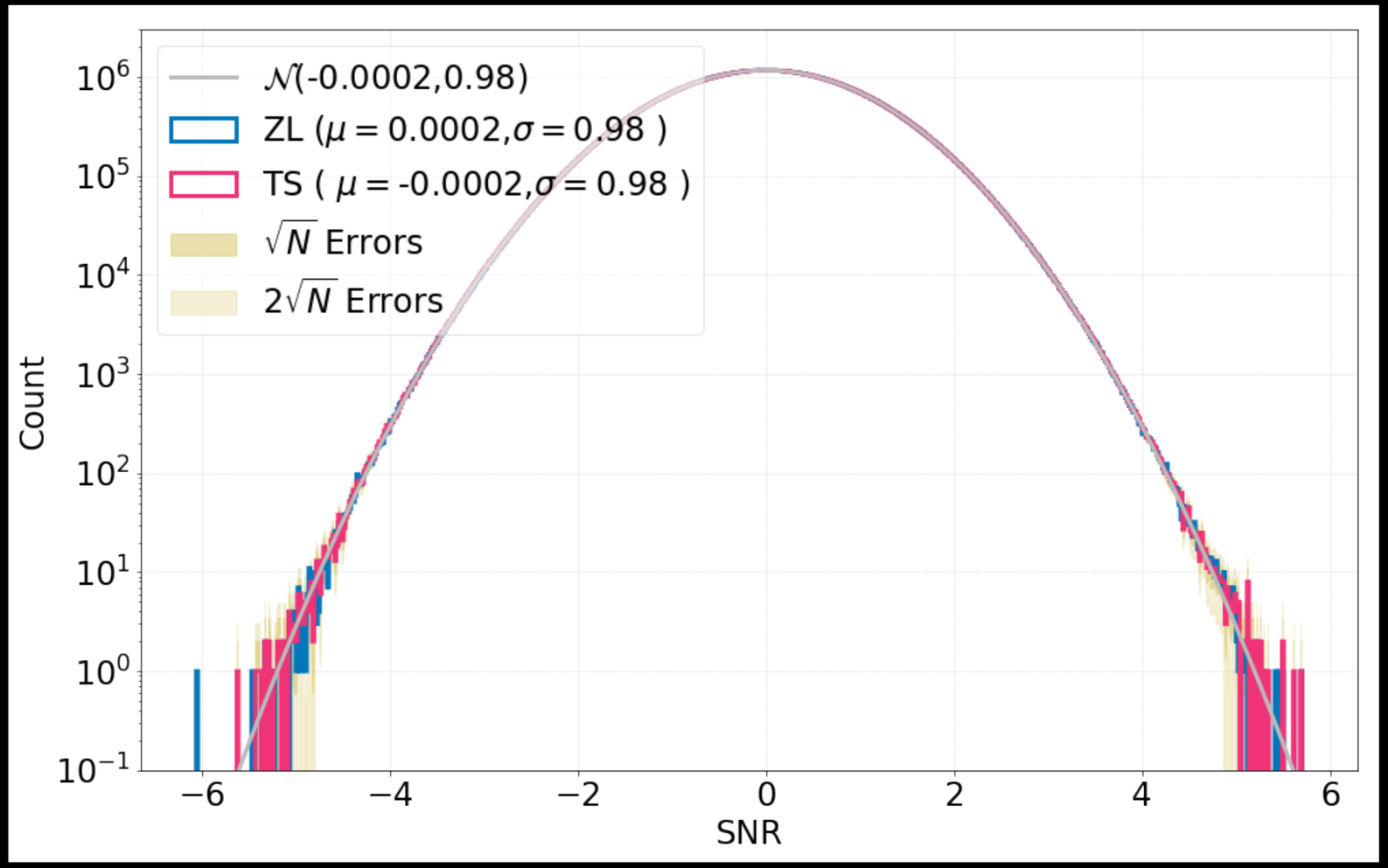

The zero-lag (ZL) data is consistent with the time-shifted (TS) data within 2-sigma error bars.

We did follow-up studies on the outlier (SNR <-6) and found no astrophysical motivated channels. This outlier is also statistically insignificant, given the trial factors corrected p-value >5%

All-Sky All-Frequency Search for SGWB

R. Abbott et al. (LVK) Phys.Rev.D 105 (2022) 10, 102001

GW data from LIGO-Virgo-KAGRA's first three observing runs (O1 + O2 + O3)

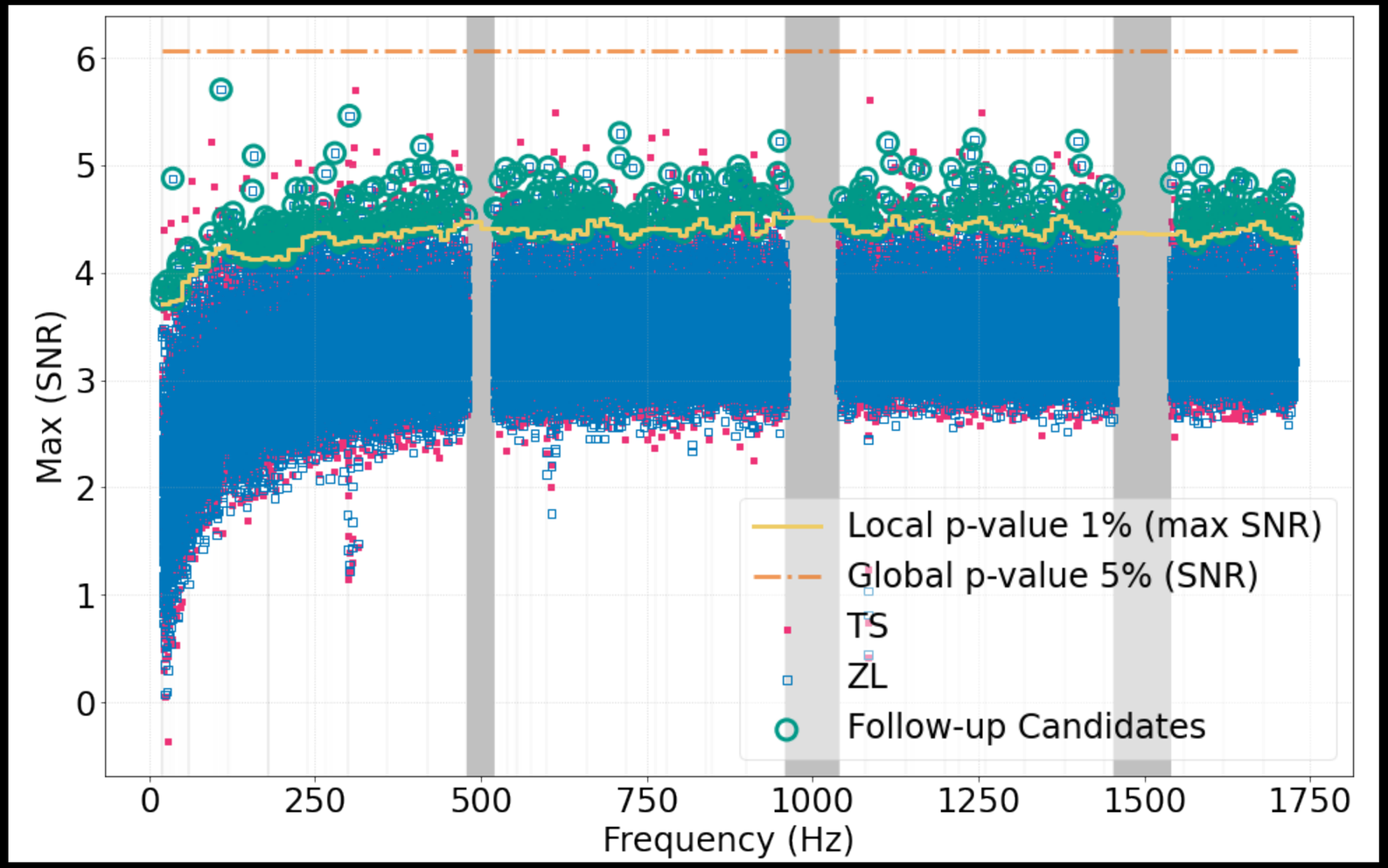

The potential (insignificant) candidates for follow-up with a more sensitive analysis are identified by comparing the distribution of max (SNR) obtained by the zero-lag run with the time-shifted run.

All-Sky All-Frequency Search for SGWB

R. Abbott et al. (LVK) Phys.Rev.D 105 (2022) 10, 102001

Given no detection, we set the first all-sky all-frequency upper limits on the SGWB strain

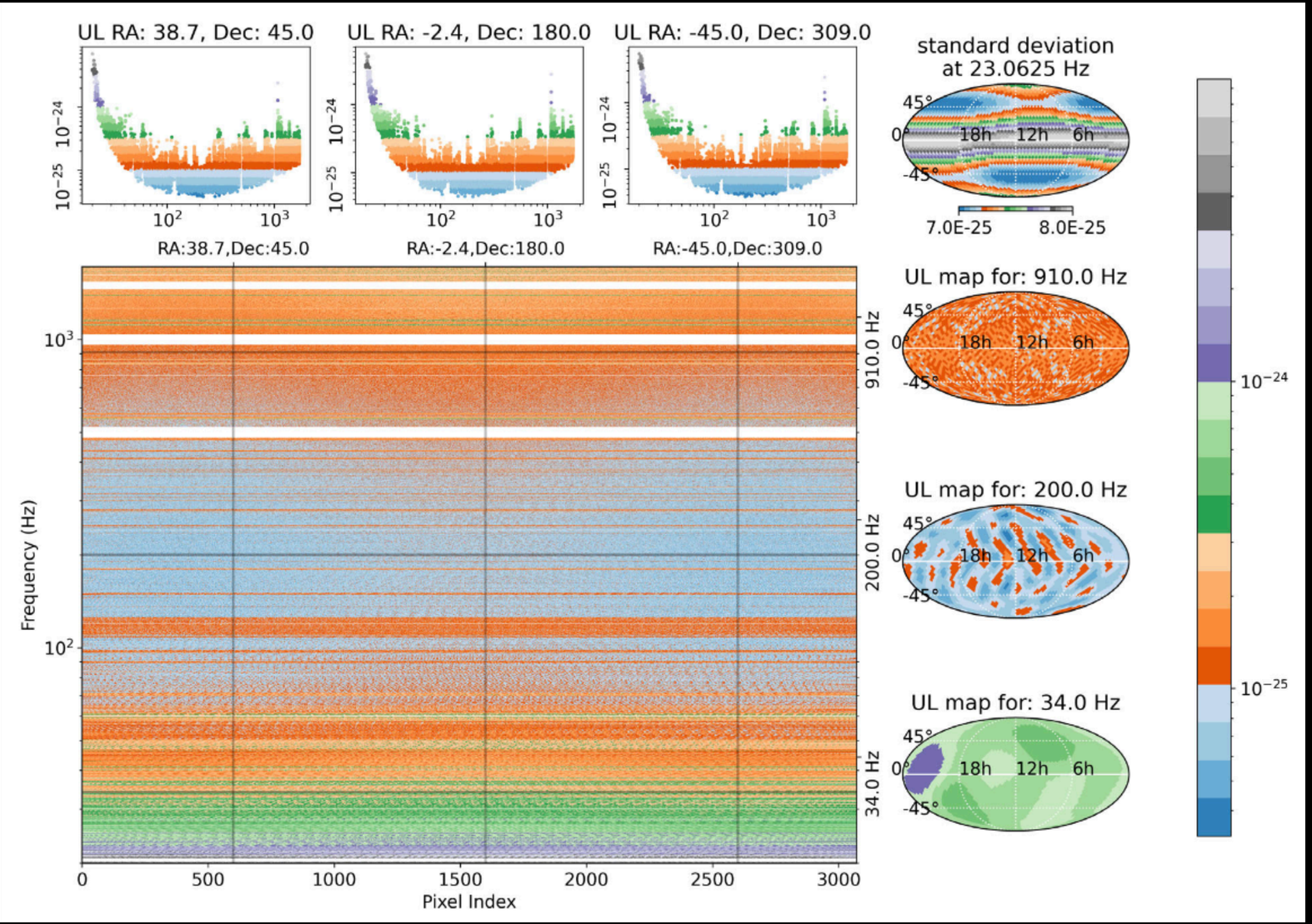

- The colour bar here denotes the range of upper limit variations.
- The vertical cross-section in this diagram shows the frequency-dependent upper limit in a particular direction.
- The Horizontal cross-sections form a map of upper limits in a particular frequency.
- Notched frequencies in a baseline appear as horizontal white bands in the plot.

All-Sky All-Frequency Search for SGWB

R. Abbott et al. (LVK) Phys.Rev.D 105 (2022) 10, 102001

Assume a power law and combine these narrowband maps to obtain the ‘usual’ broadband results

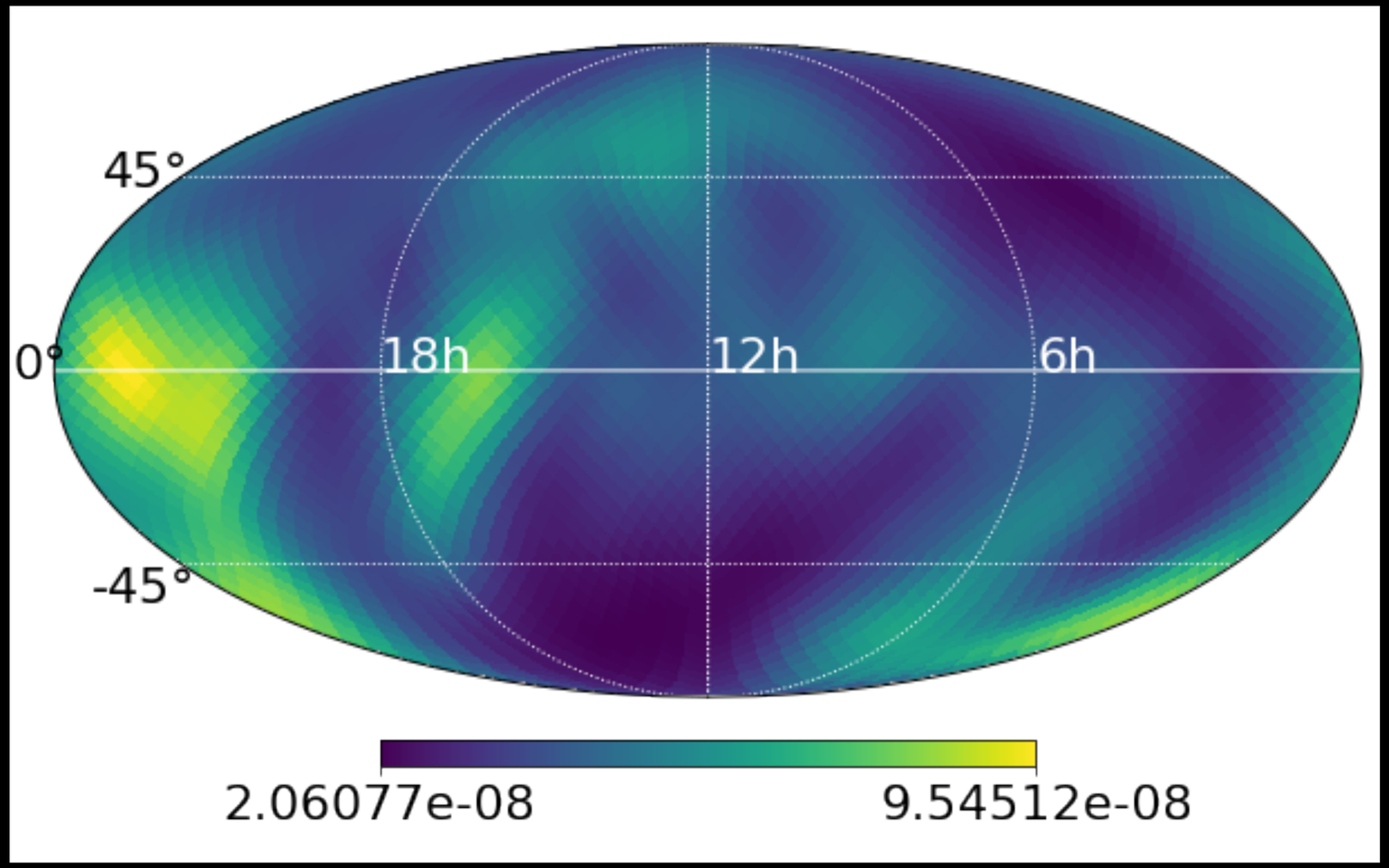

R. Abbott et al. (LVK) Phys. Rev. D 104, 022005 (2021).

All-Sky All-Frequency Search for SGWB

R. Abbott et al. (LVK) Phys.Rev.D 105 (2022) 10, 102001

Assume a power law and sum over all the directions of these narrowband maps to obtain the ‘usual’ isotropic results

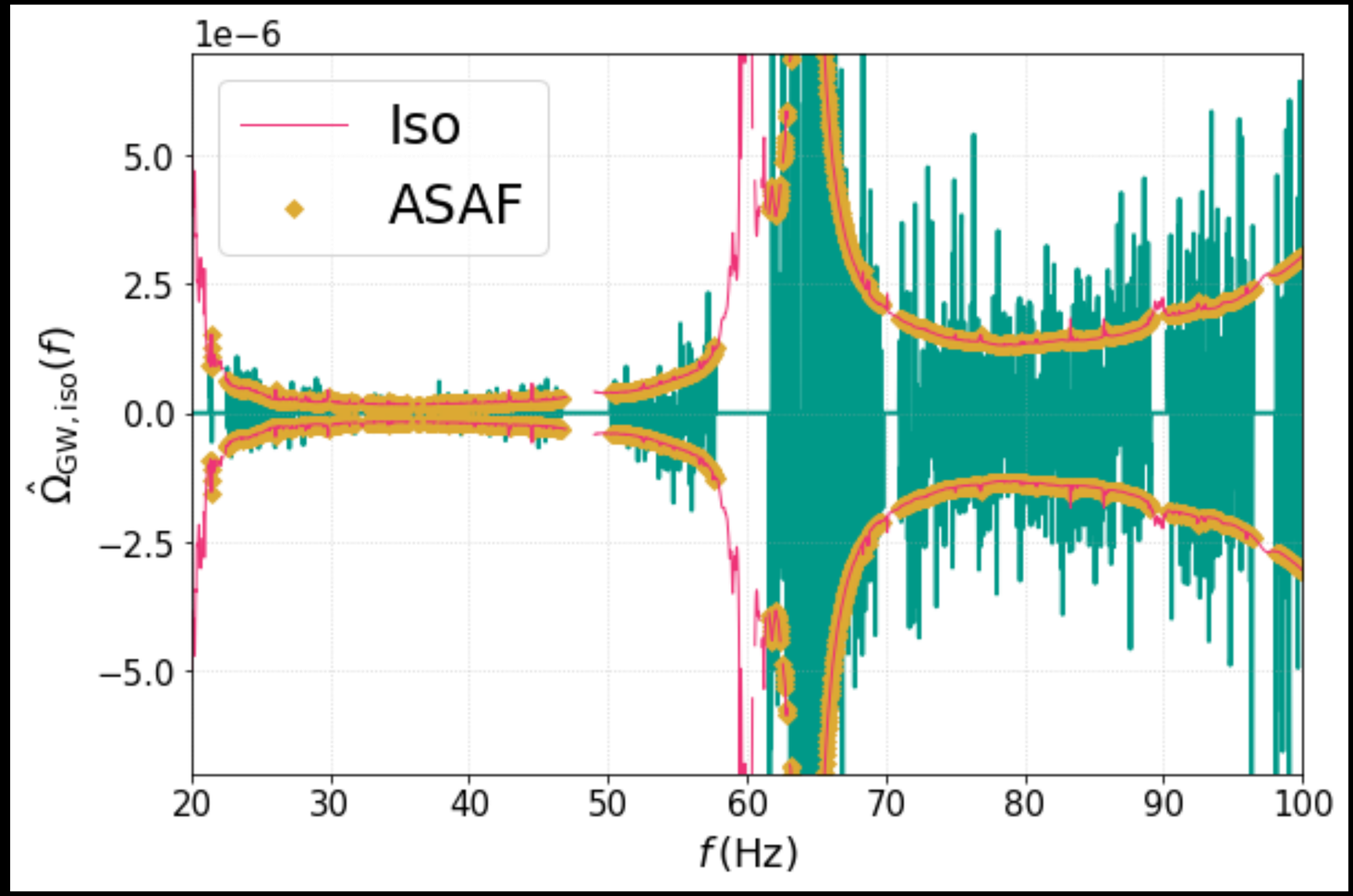

R. Abbott et al. (LVK) Phys. Rev. D 104, 022004 (2021).

SUMMARY

- New searches and techniques are opening up efficient ways to probe the dark universe.
- SGWB detection is likely in the next 3-5 years.
  - O4: May 2024 (~18-month observation).
  - O5: Start in 2026 - 2027.
- Plenty more work to do! More signals, more systems, plus dealing with real data.....